Russian Geology and Geophysics © 2019, V.S. Sobolev IGM, Siberian Branch of the RAS
Vol. 60, No. 11, pp. 1229–1246, 2019 *DOI:10.15372/RGG2019114* *Geologiya i Geofizika*

Solid Solutions of Karelianite and Eskolaite (Slyudyanka Complex, Southern Baikal Area): Genesis and a Possible Petrogenetic Indicator

L.Z. Reznitsky[a, ✉], E.V. Sklyarov[a], L.F. Suvorova[b], I.G. Barash[a]

[a] *Institute of the Earth's Crust, Siberian Branch of the Russian Academy of Sciences, ul. Lermontova 128, Irkutsk, 664033, Russia*

[b] *A.P. Vinogradov Institute of Geochemistry, Siberian Branch of the Russian Academy of Sciences, ul. Favorskogo 1a, Irkutsk, 664033, Russia*

Received 6 March 2019; accepted 22 May 2019

Abstract—A continuous solid-solution series between the end-members eskolaite (98 wt.% Cr_2O_3) and karelianite (93 wt.% V_2O_3) has been revealed in Cr–V-bearing rocks of the Slyudyanka metamorphic complex. Chromium and vanadium oxides crystallized as karelianite-eskolaite minerals during regional high-temperature prograde (granulite facies) metamorphism and participated in the formation of other Cr–V and Cr–V-bearing phases. Ferrian karelianite (up to 12 wt.% Fe_2O_3) and three-component solid solutions $Esk_{12–50}Kar_{45–60}Hem_{6–30}$ occur in metamorphic rocks that have particular protolith compositions (Fe–Kar) and in later metasomatic rocks ($(Cr, V, Fe)_2O_3$). Natural eskolaite and karelianite are discussed in terms of paragenesis, and their crystallization conditions are compared with the conditions of their laboratory synthesis.

Keywords: eskolaite, karelianite, solid solution, genesis, synthesis

INTRODUCTION

Natural Cr and V oxides of eskolaite (Cr_2O_3) and karelianite (V_2O_3) were discovered in the Outokumpu Cu–Co–Zn deposit in Finland, which has been known since the 1900s as a rich source of Cr–V mineralization. Eskolaite was found in Cr-bearing tremolite skarn, in pyrrhotite-rich sulfide ores and pyrrhotite veins, as well as in pyrrhotite-bearing quartzite next to the ore bodies (Kouvo and Vuorelainen, 1958). Karelianite occurred in disseminated and massive sulfide ores and was especially abundant in sulfide veins that crosscut the zones of disseminated ore (Long et al., 1963).

After that discovery, eskolaite was reported from various rock types and geological settings: chromitite and magnetite-ilmenite ores associated with mafic and ultramafic rocks (Moloshag et al., 1996, 1999; Erokhin, 2006; Bocharnikova and Voronina, 2008; Yang et al., 2015); kimberlites (Sobolev, 1974; Sobolev et al., 1993; Logvinova et al., 2008; Schulze et al., 2014); metasedimentary rocks (Reznitsky et al., 1988; Zhang et al., 1987; Koneva and Suvorova, 1995); hydrothermal and metasomatic rocks (Milton et al., 1976; Rumyantseva and Lapshin, 1986; Alexandre et al., 2014); and even unmetamorphosed sediments, where its origin is unclear though (Oppenheim et al., 1977; Cassedanne and Cassedanne, 1980; Karpenko and Tishchenko, 1992). In addition to terrestrial rocks, eskolaite was discovered in lunar regolith (Bogatikov et al., 2001; Mokhov et al., 2007, 2017) and has been often reported from meteorites, mainly carbonaceous chrondrite or other varieties (Ramdohr, 1977; Kimura and Ikeda, 1992; Prinz et al., 1994; Greshake and Bischoff, 1996; Barber and Scott, 2006; Ma et al., 2011; Liu et al., 2016; Nazarov et al., 2009; etc.).

Karelianite is more limited in occurrence and in diversity of its host rocks. It is known from uranium (Geffroy et al., 1964; Agrinier and Geffroy, 1969; Saint-Martin, 1977; Brodtkorb, 1982) and gold or Au–Te (Pan and Fleet, 1992; Spry and Scherbarth, 2006) fields; complex ore and pyrite deposits, where it was first found (Hoeller and Stumpfl, 1995; Sergeeva et al., 2011; Karpov et al., 2013), and from hydrothermal metasomatic rocks (Orlandi and Checchi, 1986; Rumyantseva and Lapshin, 1986; Mikhailova et al., 2006; Giuliani et al., 2008).

Karelianite and eskolaite have stoichiometric chemistry in most of occurrences, with Cr_2O_3 and V_2O_3 within a few wt.%, respectively, like other isostructural oxides (Al_2O_3 and Fe_2O_3). A solid solution (ss) series from Esk_{100} to $Esk_{50}Kar_{50}$ was found in metamorphic rocks from the Baikal region (Reznitsky et al., 1988, 1998; Koneva and Suvorova, 1995; Koneva, 2002), and the karelianite–eskolaite ss series was found in two more occurrences: the Rampura Agucha Pb–Zn–Ag deposit in India (Hoeller and Stumpfl, 1995) and the Namalulu deposit of gem tsavorite in Tanzania (Feneyrol et al., 2012). Eskolaite and karelianite with a high percentage of the hematite component and Al eskolaite are very rare, while karelianite with notable amounts of Al_2O_3 has never been found.

✉ Corresponding author.
E-mail adress: garry@crust.irk.ru (L.Z. Reznitsky)

The known mineralogy of the Slyudyanka Cr–V-bearing granulite complex includes an almost complete eskolaite–karelianite ss series, ferrian karelianite, and a unique three-component ss series of hematite–eskolaite–karelianite. We describe the mineralogy of the complex and present a synopsis of natural settings of eskolaite and karelianite and their solid solutions, as well as experimental results on synthesis of the two minerals. The results can be used to check the possibility for using eskolaite and karelianite as petrogenetic indicators.

OCCURRENCE OF Cr–V MINERALIZATION

The setting of Cr–V mineralization in the southern Baikal region was discussed in many earlier publications (e.g., (Vasiliev et al., 1981; Konev et al., 2001; Reznitsky et al., 2011)) and is described only briefly below.

Quartz-diopside rocks bearing Cr and V phases belong to the Slyudyanka Group, a major stratigraphic unit in the Slyudyanka metamorphic complex that comprises highest-grade granulite rocks of the Khamar-Daban terrane on the folded periphery of the Siberian craton. They are metamorphosed siliceous-dolomite chemogenic sediments with variable percentages of calcite. Among the metamorphites banded rocks, consisting of alternating bands of quartz and diopside compositions, dominate. Separate layers of quartzite, diopside and calciphyres are present also.

Some varieties containing rock-forming fluorapatite are classified as metaphosphorites and some others, much less abundant but often found, are rich in Cr and V. The Cr–V mineralization is presented by diverse Cr–V-bearing minerals and Cr–V phases: pyroxene, amphibole, garnet, tourmaline, dioctahedral and trioctahedral micas, chlorite, titanite, sulfides, complex and simple oxides including those of the karelianite–eskolaite series.

The quartz-diopside layers of different thicknesses, all with sporadic Cr–V mineralization, make up 6–7 vol.% of the Slyudyanka Group and lie at several stratigraphic levels. The persistent association of Cr–V mineralization with a certain lithological and petrographic type of metasedimentary rocks indicates that Cr and V were present in the protolith rather than being incorporated by metamorphic or metasomatic reactions. The chemogenic origin of the protolith, with minor clastic and clay components, can be inferred from low contents of Fe, Ti, Mn, Na, and K oxides (most often within 0.*n* wt.%) and Al_2O_3 (≤0.2–1 wt.%) at quite a large share of carbonates in the Slyudyanka quartz-diopside rocks. Cr and V mineralization may be a consequence of synsedimentary volcanism: Cr and V were carried into the basin by submarine hydrotherms, concurrently with P and Si, in lulls between volcanic activity events. Igneous rocks appear as metabasaltic sills in the Slyudyanka section (Vasiliev et al., 1981; Konev et al., 2001; Shkol'nik et al., 2011).

METHODS

In order to create a representative analytical database, karelianite and escolaite, which are accessories in the Slyudyanka metamorphic rocks, were analyzed in thin sections and in heavy mineral concentration samples; in the latter case, the minerals were extracted by electromagnetic and heavy liquid separation. Many analytical data were collected previously during studies of other newly discovered Cr–V phases (Reznitsky et al., 1988, 1998; Konev et al., 2001; Secco et al., 2008). Most of analyses used in this study were obtained at the Analytical Center for Isotope and Geochemical Research of the Vinogradov Institute of Geochemistry (Irkutsk), on a *Jeol JXA-8200* superpobe analyzer. The instrument consists of a high-resolution scanning electron microscope (SEM) and a combined wave- and energy-dispersive (WD/ED) electron probe microanalyzer (EPMA), with five wavelength dispersive X-ray spectrometers (WDS) and an energy dispersive X-ray spectrometer (EDS) with a SiLi detector. The structure of mineral grains was examined in secondary- and backscattered-electron images on a raster electron microscope, and the distribution of elements was mapped at their characteristic X-ray wavelengths. Element contents were measured using wave-dispersive spectrometers at an accelerating voltage of 20 kV, a beam current of 20 nA, a beam diameter of 1 μm, and a counting time of 10 s on peak; the background was measured on both sides of the line peak, for 5 s. Matrix correction was performed using the ZAF procedure with the built-in software. The results were checked against natural and synthetic standards certified as reference materials at the V.S. Sobolev Institute of Geology and Mineralogy (Novosibirsk): Cr_2O_3 (Cr), V_2O_5 (V), Fe_2O_3 (Fe), ZnS (Zn), GF-55 ilmenite (Ti), diopside (Mg, Ca, and Si), and Mn-garnet (Mn).

RESULTS

The oxide minerals of the karelianite–eskolaite solid solution series are present as accessories in quartz-bearing varieties of quartz-diopside rocks, less frequently occur in quartz-free diopsidite, and are absent from quartz-free magnesian marble and calciphyre layers. Apatite-bearing quartz-diopside rocks (metaphosphorite) commonly lack karelianite–eskolaite minerals and Cr–V mineralization.

The karelianite–eskolaite phases are of three groups according to mineral chemistry: (i) low-Fe almost complete karelianite–eskolaite join; (ii) three-component hematite–karelianite–eskolaite series found in a few samples (out of more than 100), and (iii) ferrian karelianite in a single sample. The limit to distinguish between low-Fe and ferrian minerals is assumed to be at ~5 wt.% Fe_2O_3, which is the highest content observed in eskolaite coexisting with chromitie in most of the Slyudyanka rocks. Fe_2O_3 very rarely exceeds 5 wt.% in natural karelianite and eskolaite, and even in chromitite or pyrite ores.

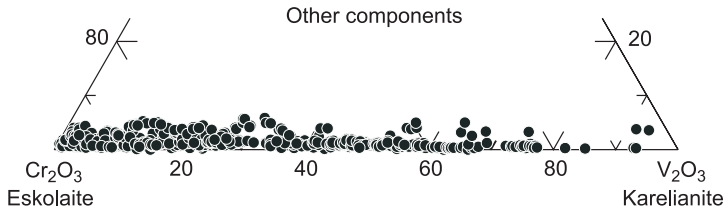

Fig. 1. Ternary diagram for the eskolaite–karelianite join.

The V_2O_3–Cr_2O_3 join (Fig. 1, Table 1) includes highly variable minor oxides: up to 0.0*n* wt.% or below the detection limit; totally no higher than 1.5–3 mol.%, or less often ≥3 mol.%. Most of the compositions range from Esk_{100} to Kar_{80} and rarely approach pure karelianite. The karelianite–eskolaite minerals in quartz and inclusions in Cr–V minerals differ in structure and morphology. Quartz most often hosts euhedral and subhedral eskolaite and karelianite microcrystals (30–50 to 100–150 μm, rarely larger) of hexagonal platy or less often columnar short- and long-prismatic or flat elongate shapes (Fig. 2). Some crystals have pseudotetragonal faceting, possibly, produced by separate faces of hexagonal prisms. The crystal morphology shows no correlation with Cr or V prevalence which discriminates between eskolaite and karelianite. The crystals are generally unzoned, with ≤1–3 wt.% core–rim Cr and V variations, without distinct trends; Cr/V ratios may vary in different crystals within a specimen but generally correlate with those in bulk rock.

Karelianite–eskolaite inclusions more or less frequently occur in almost all Cr–V and Cr–V-bearing minerals, commonly as anhedral grains, unlike the inclusions in quartz. Most interesting are those in clinopyroxene (main rock-forming silicate) because they often display oxide–silicate reaction relations which have petrogenetic implications.

The eskolaite inclusions in clinopyroxene are mostly anhedral and are surrounded with aureoles of high Cr and (or) V contents. More or less bright green aureoles of Cr–V pyroxene appear around karelianite–eskolaite grains in colorless or pale green diopside (with low Cr and V) in thin sections and even in grains under a binocular (Fig. 3). Oxide grains look like being "dissolved" in pyroxene, especially in the presence of a few closely spaced microcrysts that resemble remnants of disintegrated and incompletely "dissolved" grains. There are also some particular structures which may result from partial recrystallization of karelianite–eskolaite. Lath-like and acicular microcrysts of karelianite–eskolaite either surround anhedral relict grains or cluster in pyroxene where mark the original oxide grains (Fig. 4*A, B*). Some clusters of lath- and needle-shaped microcrystals have sharp boundaries which apparently follow

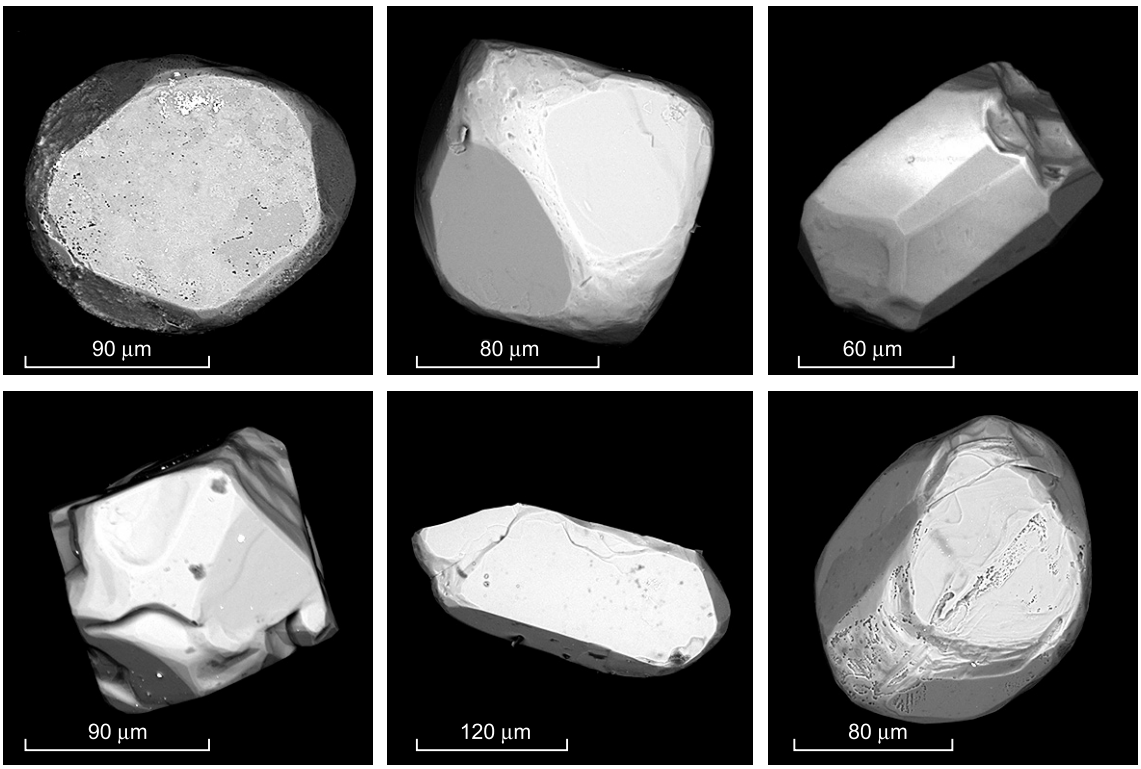

Fig. 2. Morphological types of karelianite–eskolaite microcrystals. SEM images.

Table 1. Selected EMPA data for oxides of escolaite-karelianite (Cr_2O_3–V_2O_3) join from metamorphic rocks of the Slyudyanka complex

Oxide	1	2	3	4	5	6	7	8	9	10	11	12	13	14	15	16
SiO_2, wt.%	0.05	0.08	0.01	0.29	0.01	0.01	0.00	0.04	0.00	0.04	0.07	0.01	0.00	0.00	0.00	0.00
TiO_2	0.18	0.00	0.09	0.01	0.06	0.28	0.09	0.07	0.07	0.08	0.06	0.08	0.20	0.14	0.10	0.23
Al_2O_3	0.98	0.29	0.91	0.44	0.84	0.88	0.85	0.82	0.52	0.95	0.47	0.94	0.46	0.44	0.34	0.40
Cr_2O_3	98.01	96.87	94.64	92.00	90.74	88.02	86.43	84.67	82.71	80.56	78.26	76.23	74.22	72.44	70.22	68.09
V_2O_3	0.49	2.98	3.76	6.47	7.23	8.61	11.55	14.13	15.95	17.32	19.77	21.91	24.15	25.82	28.72	29.70
Fe_2O_3	0.14	0.12	0.48	0.27	1.00	1.46	1.16	0.03	0.51	0.94	0.73	1.12	0.63	0.61	0.91	0.85
MnO	0.14	0.04	0.11	0.01	0.07	0.13	0.08	0.07	0.07	0.07	0.00	0.04	0.10	0.12	0.12	0.09
MgO	0.07	0.07	0.03	0.08	0.02	0.12	0.05	0.00	0.09	0.07	0.05	0.08	0.23	0.14	0.12	0.19
CaO	0.19	0.06	0.03	0.29	0.20	0.00	0.14	0.54	0.00	0.19	0.23	0.03	0.00	0.00	0.00	0.01
ZnO	0.03	0.01	0.00	0.00	0.04	0.02	0.00	0.00	0.02	0.04	0.00	0.00	0.00	0.01	0.00	0.00
Total	100.28	100.52	100.06	99.86	100.21	99.53	100.35	100.37	99.94	100.26	99.64	100.44	99.99	99.72	100.53	99.56
Atoms per formula unit (based on three oxygens)																
Si	0.001	0.002	–	0.007	–	–	–	0.001	–	0.001	0.002	–	–	–	–	–
Ti	0.003	–	0.002	–	0.001	0.005	0.002	0.001	0.001	0.002	0.001	0.001	0.004	0.003	0.003	0.004
Al	0.029	0.009	0.027	0.013	0.025	0.026	0.025	0.024	0.015	0.028	0.014	0.028	0.014	0.013	0.010	0.012
Cr	1.945	1.923	1.883	1.834	1.804	1.759	1.714	1.678	1.648	1.596	1.563	1.507	1.475	1.444	1.388	1.359
V	0.010	0.060	0.076	0.131	0.146	0.175	0.232	0.284	0.322	0.348	0.400	0.439	0.487	0.522	0.576	0.601
Fe	0.003	0.002	0.009	0.005	0.019	0.028	0.022	0.001	0.010	0.018	0.014	0.021	0.012	0.012	0.017	0.016
Mn	0.003	0.001	0.002	–	0.002	0.003	0.002	0.002	0.001	0.001	–	0.001	0.002	0.003	0.003	0.002
Mg	0.002	0.003	0.001	0.003	0.001	0.004	0.002	–	0.003	0.003	0.002	0.003	0.009	0.005	0.004	0.007
Ca	0.005	0.001	0.001	0.008	0.005	–	0.004	0.014	–	0.005	0.006	0.001	–	–	–	–
Zn	0.001	–	–	–	0.001	–	–	–	–	0.001	–	–	–	–	–	–
Total	2.002	2.001	2.001	2.001	2.004	2.000	2.003	2.005	2.000	2.003	2.002	2.001	2.003	2.002	2.001	2.001
Components, mol.%																
Eskolaite	97.2	96.1	94.1	91.7	90.1	87.9	85.6	83.7	82.4	79.7	78.1	75.3	73.7	72.1	69.4	67.9
Karelianite	1.5	3.0	3.9	6.5	7.3	8.7	11.6	14.2	16.1	17.4	20.0	22.9	24.3	26.1	28.8	30.5
Others	1.3	0.9	2.0	1.8	2.6	3.4	2.8	2.1	1.5	2.9	1.9	1.8	2.0	1.8	1.8	1.6

(*continued on next page*)

the contours of the primary karelianite–eskolaite crystals (Fig. 4*C, D*).

Chemical analyses of the aureoles and karelianite–eskolaite inclusions reveal notable difference in Cr and V patterns. Generally, Cr and V concentrations decrease gradually from the contacts with karelianite–eskolaite toward the aureole margin (Fig. 5*A*). Cr_2O_3 often decreases rapidly and zeroes down away from the inclusions, while V_2O_3 changes smoothly and in different ways: it may be evenly distributed over the grain (Fig. 5*B*) or be lower near the karelianite–eskolaite inclusion than away from it (Fig. 6*A*). Unlike the inclusions in quartz, the remnant karelianite–eskolaite oxide in clinopyroxene is often inhomogeneous, which is clearly seen in large inclusions of 50–100 μm or more. Panels *A* and *B* of Fig. 6 illustrate, respectively, vanadium depletion near the inclusion margin and a complex pattern with Cr decrease and V increase toward the margin (notable Cr/V change). As the Cr and V percentages in pyroxene increase, the aureoles become less contrasting, and the contrasts near inclusions disappear in pyroxenes with compositions close to kosmochlor–natalyite $Na(Cr,V)Si_2O_6$. The latter quite often enclose numerous inclusions or large aggregates of relict karelianite–eskolaite (Fig. 7). Note that low-Cr karelianite with >90 mol.% V_2O_3 is restricted to inclusions in natalyites which almost lack Cr and Mg.

Occasionally oxide inclusions in pyroxene are surrounded with goldmanite-uvarovite garnet (Fig. 8*A*), while the Cr and V patterns remain different: Cr is almost zero beyond the garnet rim and V is distributed uniformly in all three minerals, being quite low in garnet. Structures of this kind more often occur in Cr–V-bearing epidote than in pyroxene, where Cr and V likewise behave in different ways (Fig. 8*B*): Cr in eskolaite markedly decreases toward the inclusion margin and is low in garnet and epidote; V contents are relatively high in garnet and notable and evenly distributed in epidote.

Karelianite–eskolaite inclusions can also occur in other minerals, besides quartz and pyroxene: garnet, tourmaline, and spinel, where cause no influence on the distribution of Cr and V in garnet and on (Cr–V–Al) growth zonation in Cr–V-tourmaline. They commonly occur as euhedral and subhedral microcrystals in sulfospinels of the kalininite–florensovite series (Fig. 9*A*) or are rarely surrounded by kalin-

Table 1 (*continued*)

Oxide	17	18	19	20	21	22	23	24	25	26	27	28	29	30	31	32	33
SiO_2, wt.%	0.00	0.00	0.00	0.00	0.00	0.00	0.00	0.03	0.00	0.00	0.00	0.00	0.03	0.04	0.00	0.04	0.05
TiO_2	0.12	0.39	0.26	0.17	0.19	0.19	0.19	0.12	0.33	0.27	0.09	0.30	0.07	0.08	0.00	0.22	0.00
Al_2O_3	0.30	0.47	0.72	0.37	0.36	0.33	0.34	0.51	0.29	0.29	0.12	0.23	0.18	0.16	0.00	0.07	0.02
Cr_2O_3	66.85	65.67	61.80	59.85	56.89	54.81	52.98	50.05	47.70	44.87	42.91	40.33	38.64	36.47	25.94	22.82	6.73
V_2O_3	29.08	32.91	34.00	39.10	41.52	43.54	45.76	48.87	51.09	51.87	55.86	58.00	61.47	62.49	73.15	76.56	93.35
Fe_2O_3	4.10	0.18	2.70	0.49	0.46	0.43	0.44	0.53	0.42	2.00	0.30	0.59	0.00	0.04	0.55	0.40	0.24
MnO	0.07	0.04	0.02	0.08	0.05	0.10	0.05	0.04	0.06	0.04	0.07	0.02	0.00	0.00	0.02	0.00	0.00
MgO	0.03	0.18	0.10	0.06	0.09	0.11	0.10	0.02	0.18	0.09	0.27	0.14	0.08	0.12	0.76	0.17	0.07
CaO	0.00	0.02	0.00	0.00	0.00	0.00	0.00	–	0.00	0.01	0.00	0.05	0.04	0.02	0.01	0.01	0.00
ZnO	0.04	0.00	0.01	0.01	0.00	0.00	0.00	0.01	0.00	0.00	0.01	0.04	0.00	0.00	0.00	0.00	0.00
Total	100.59	99.86	99.61	100.13	99.56	99.51	99.86	100.18	100.07	99.44	99.63	99.70	100.51	99.42	100.43	100.29	100.46
Atoms per formula unit (based on three oxygens)																	
Si	–	–	–	–	–	–	–	0.001	–	–	–	–	0.001	0.001	–	0.001	0.001
Ti	0.002	0.007	0.005	0.003	0.004	0.004	0.003	0.002	0.006	0.005	0.002	0.006	0.001	0.002	–	0.004	–
Al	0.009	0.014	0.021	0.011	0.011	0.010	0.010	0.015	0.008	0.009	0.003	0.007	0.005	0.005	–	0.002	0.001
Cr	1.324	1.305	1.231	1.187	1.134	1.093	1.052	0.989	0.944	0.895	0.854	0.801	0.761	0.726	0.511	0.450	0.132
V	0.584	0.663	0.687	0.786	0.839	0.880	0.922	0.980	1.026	1.049	1.127	1.168	1.228	1.262	1.460	1.530	1.859
Fe	0.077	0.003	0.051	0.009	0.009	0.008	0.008	0.010	0.008	0.038	0.006	0.011	–	0.001	0.010	0.008	0.004
Mn	0.001	0.001	–	0.002	0.001	0.002	0.001	0.001	0.001	0.001	0.001	–	–	–	–	–	–
Mg	0.001	0.007	0.004	0.002	0.003	0.004	0.004	0.002	0.007	0.003	0.010	0.005	0.003	0.005	0.028	0.006	0.003
Ca	–	0.001	–	–	–	–	–	0.001	–	–	–	0.001	0.001	0.001	–	–	–
Zn	0.001	–	–	–	–	–	–	–	–	–	–	0.001	–	–	–	–	–
Total	1.999	2.001	1.999	2.000	2.001	2.001	2.000	2.000	2.000	2.000	2.003	2.000	1.999	2.002	2.009	2.000	1.999
Components, mol.%																	
Eskolaite	66.2	65.3	61.6	59.4	56.7	54.6	52.6	49.5	47.2	44.7	42.6	40.0	38.0	36.2	25.4	22.5	6.6
Karelianite	29.2	33.2	34.4	39.3	42.0	44.0	46.1	49.0	51.3	52.4	56.3	58.4	61.4	63.0	72.6	76.5	91.5
Others	4.6	1.5	4.0	1.3	1.3	1.4	1.3	1.5	1.5	2.9	1.1	1.6	0.6	0.8	2.0	1.0	1.9

Note. All iron quoted as Fe_2O_3.

inite–florensovite in clinopyroxene (Fig. 9*B*). Relative percentages of Cu–Zn and Sb–Cr in sulfospinel are most often variable but the inclusions do not affect Cr/V ratios.

Ferrian karelianite was found in a single sample of particular calciphyre, which has low Mg contents and lacks forsterite, dolomite, and quartz, unlike ordinary calciphyre which forms layers in quartz-diopside rocks. Its mineralogy includes calcite, clinopyroxene, spinel, karelianite, and oxyvanite. The bulk rock content of V is much higher than that of Cr, but V prevails in pyroxene and spinel. Karelianite and oxyvanite form either separate microcrystals or alternating bands in composite layer-by-layer grown crystals (Fig. 10). Major oxides are 3 to 10 wt.% TiO_2 and 2–3 wt.% Fe_2O_3 in oxyvanite and 6 to 12 wt.% Fe_2O_3 (Fig. 11, Table 2) and 0.7 to 1.5 wt.% MgO in karelianite; this Mg content is uncommon to karelianite–eskolaite in other parageneses.

The hematite–eskolaite–karelianite solid solutions are present in quartz-diopside rocks subjected to postmetamor-

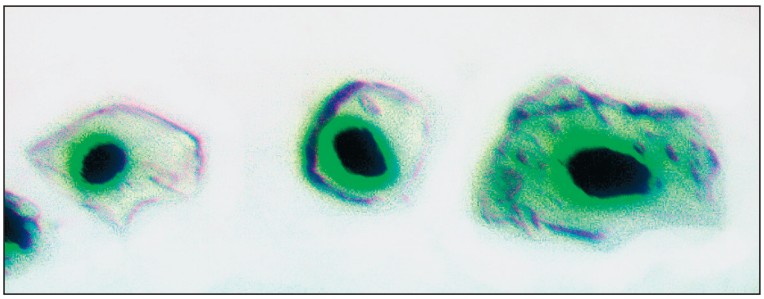

Fig. 3. Karelianite–eskolaite inclusions in diopside. See a green V- and Cr-rich pyroxene rim around the inclusions. Grain sizes 100–200 μm.

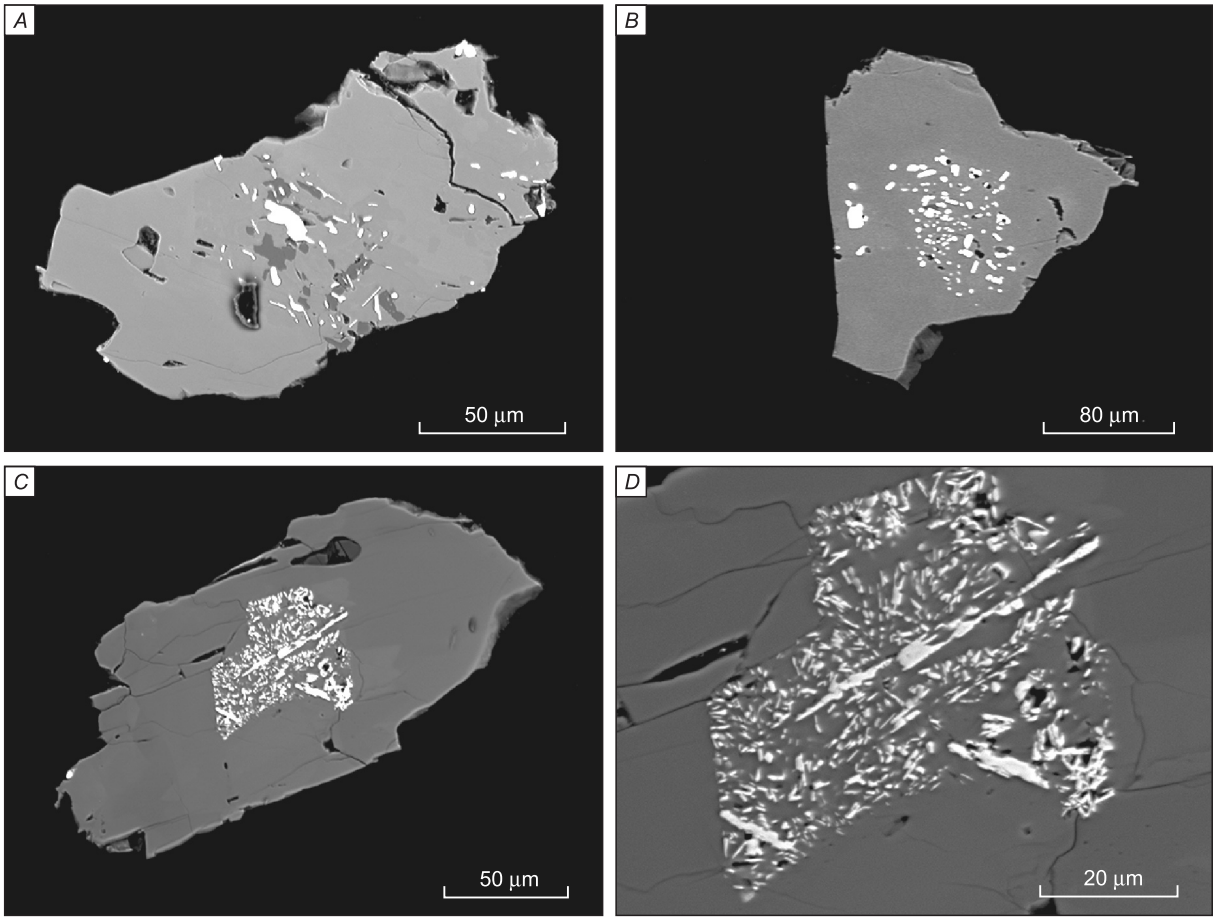

Fig. 4. Recrystallized lath-like karelianite–eskolaite inclusions in pyroxene. *A*, around a relict grain; *B*, newly formed microcrystals; *C*, cluster of microcrystals that repeats the contours of the primary inclusion; *D*, fragment. BSE image.

phic contact metasomatism. In addition to newly formed minerals (scapolite, feldspar), some silicate and oxide metasomatic minerals retain the Cr–V specificity but their composition has been markedly changed. Pyroxenes include a notable amount of the gedenbergite component while Cr–V-garnets contain much andradite. There are three-component spinels of magnetite–chromite–coulsonite series (Reznitsky et al., 2005). The hematite component in karelianite–eskolaite reaches 30 mol.% (Fig. 11, Table 3). The compositional variability of Cr–V minerals is especially prominent in metasomatic rocks with variable Fe contents (Fig. 10).

DISCUSSION

Almost all minerals in the Slyudyanka Cr–V-bearing metamorphic rocks enclose karelianite–eskolaite oxides which crystallized as the earliest phases during prograde metamorphism. Obviously, Cr and V were present in the protolith rather than resulting from metamorphic or metasomatic alteration, but their mode of occurrence remains poorly constrained. The ways of Cr and V accumulation in sediments have been largely discussed in the literature (Pan and Fleet, 1992; Hoeller and Stumpfl, 1995; Spry and Scherbarth, 2006; Giuliani et al., 2008; Feneyrol et al., 2012; etc.). Chromium is mainly carried by clastic heavy fractions while vanadium can accumulate together with organic components more often than Cr. Organic carbon from the sedimentary protolith can appear as graphite in the metamorphics, but the Slyudyanka quartz-diopside rocks are free from graphite. Finally, Cr and V can adsorb on clay minerals, which may be relevant for the varieties containing Al-bearing phases (micas, tourmaline, epidote). Most of the Slyudyanka quartz-diopside rocks have low Al contents, which however does not contradict the presence of clay minerals in the protolith. Most likely, Cr and V accumulated in the protolith together with carbonates in the form of complex oxide–hydroxides or Cr–V salts of variable compositions with high-valent Cr and V.

Dehydration and reduction to R_2O_3, as well as reactions with other minerals, were possible at ~500–600 °C and higher. The reaction with dolomite led to the formation of magnesiochromite–magnesiocoulsonite spinels: $(Cr,V)_2O_3 + CaMg(CO_3)_2 = Mg(Cr,V)_2O_4 + CaCO_3 + CO_2$. The possi-

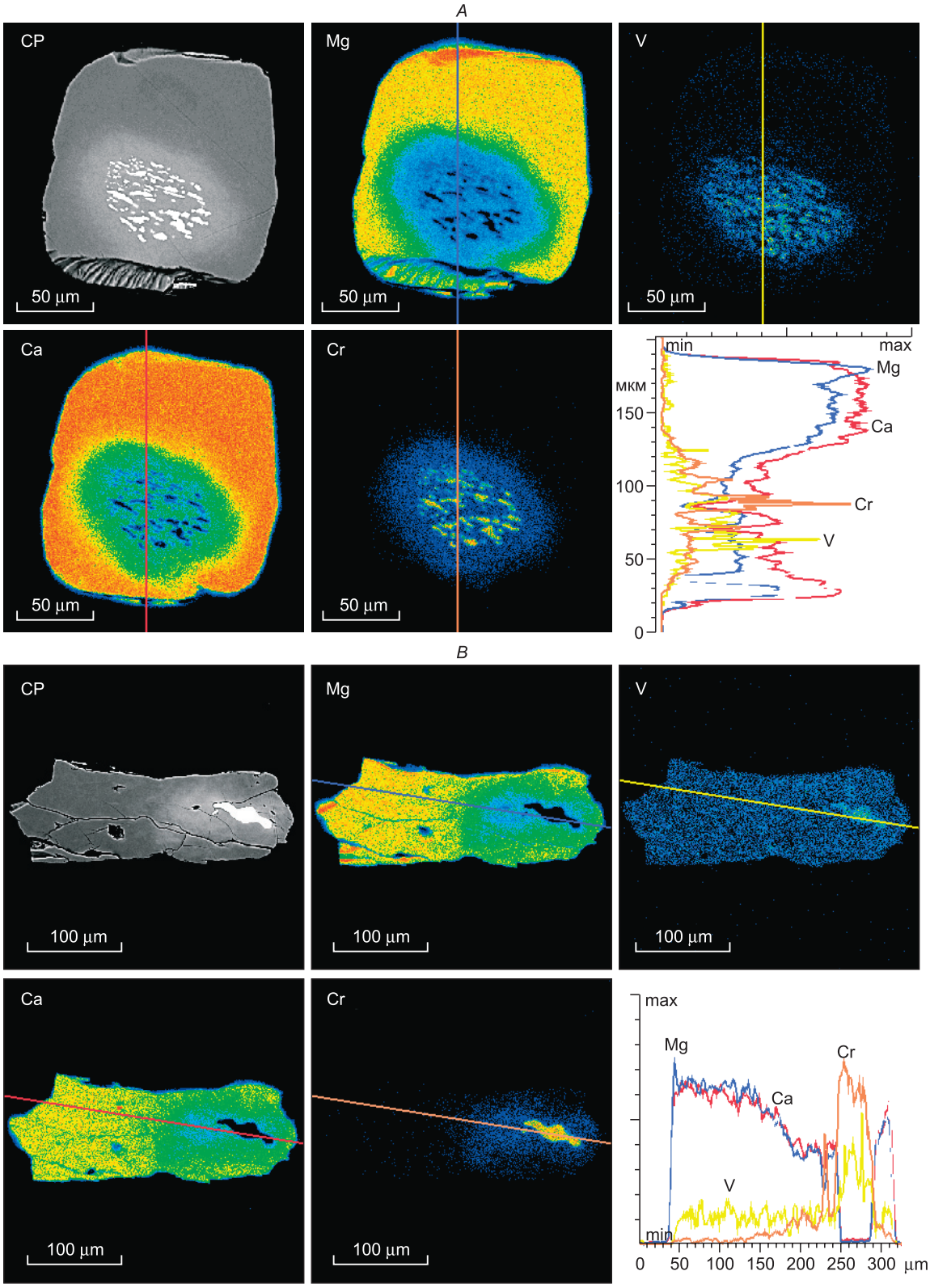

Fig. 5. Distribution of Cr, V and related Mg and Ca in diopside around karelianite–eskolaite inclusions. *A*, markedly low Cr and V contents around a cluster of newly formed crystals, behind the zone of karelianite–eskolaite microinclusions; *B*, Cr content decreasing markedly (to 0.0n%) away from a relict inclusion in pyroxene, at uniform distribution of V. BSE images (CP) and X-ray maps of Mg, Ca, Cr and V.

Table 2. Selected EMPA data for ferrian karelianite

Oxide	1	2	3	4	5	6
TiO_2, wt.%	0.13	0.00	0.51	0.25	0.54	0.00
Al_2O_3	0.04	0.34	0.00	0.04	0.01	0.19
Cr_2O_3	0.58	1.01	1.01	1.63	2.20	1.70
V_2O_3	91.93	89.56	88.15	87.19	85.95	84.97
Fe_2O_3	6.60	8.16	9.78	10.08	11.14	12.01
MgO	1.19	1.30	0.71	0.81	0.77	0.52
	100.47	100.37	100.16	100.00	100.61	99.39
Atoms per formula unit (based on three oxygens)						
Ti	0.002	–	0.010	0.005	0.010	–
Al	0.001	0.010	–	0.001	–	0.006
Cr	0.011	0.010	0.020	0.032	0.043	0.034
V	1.831	1.785	1.764	1.750	1.715	1.715
Fe	0.123	0.153	0.174	0.190	0.209	0.228
Mg	0.040	0.048	0.026	0.030	0.029	0.019
	2.008	2.006	1.994	2.008	2.006	2.002
Components, mol.%						
Eskolaite	0.5	0.9	1.0	1.6	2.1	1.7
Karelianite	91.2	88.5	88.5	87.1	85.5	85.7
Hematite	6.1	7.6	8.7	9.5	10.4	11.4
Others	2.2	3.0	1.8	1.8	2.0	1.2

Note. All iron quoted as Fe_2O_3. SiO_2, CaO, ZnO are below detection limit (0.01–0.02 wt.%).

bility of this reaction is confirmed by the absence of karelianite–eskolaite in dolomite mineral assemblages and the presence of interstitial calcite between spinel grains. The direct reaction may have produced also garnets of the goldmanite–uvarovite series in rocks bearing calcite and quartz: $(Cr,V)_2O_3 + 3CaCO_3 + 3SiO_2 = Ca_3(Cr,V)_2Si_3O_{12} + 3CO_2$. After the reaction, excess karelianite–eskolaite remains enclosed in spinel and garnet, but the host minerals do not change their composition around the inclusions because they have the same Cr/V ratios as in karelianite–eskolaite (Fig. 12).

The relation of karelianite–eskolaite with clinopyroxene is different: Cr and V incorporate into diopside by heterovalent Tchermak's or aegirine-jadeite substitutions: $R^{3+}_{VI}R^{3+}_{IV} \rightarrow$ MgSi and $NaR^{3+}_{VI} \rightarrow$ CaMg, respectively (R^{3+} – $(Cr,V)^{3+}$ in this case). The tchermakite component in pyroxene is very limited even at the granulite facies temperatures, while the aegirine-jadeite substitution is more feasible and is found in the Slyudyanka and most of other natural Cr(V)-bearing clinopyroxenes (Reznitsky et al., 2011). Aegirine-jadeite substitution requires the presence of Na, which is low in most of quartz-diopside varieties (0.0*n* to 0.2–0.3 wt.%). Some Na input was presumably possible when the complex underwent weak to moderate metasomatism after the climax of the Slyudyanka regional metamorphism. The input of Na may have been responsible for the upset eskolaite–kareli-

Table 3. Selected EMPA data for oxide minerals of the hematite–eskolaite–karelianite Fe_2O_3–Cr_2O_3–V_2O_3 series from the Slyudyanka complex

Oxide	1	2	3	4	5	6	7	8	9	10	11	12	13	14	15	16
TiO_2, wt.%	0.43	0.54	0.62	0.66	1.18	1.03	1.42	1.55	1.48	2.17	2.19	1.77	1.95	1.93	2.02	2.11
Al_2O_3	0.57	0.43	0.25	0.00	0.06	0.00	0.00	0.00	0.00	0.07	0.08	0.05	0.00	0.04	0.05	0.07
Cr_2O_3	55.80	45.70	30.68	26.53	23.19	21.73	19.16	17.28	15.80	13.99	13.27	16.62	13.23	13.50	13.05	11.68
V_2O_3	36.26	44.91	58.57	59.65	59.78	59.05	59.96	57.99	59.00	58.00	57.87	54.25	53.93	54.93	52.64	52.89
Fe_2O_3	6.66	8.20	9.74	12.89	14.93	17.37	18.34	21.86	22.25	23.87	24.18	25.90	26.89	28.15	30.95	31.19
FeO	0.10	0.19	0.33	0.46	0.94	0.74	1.09	1.23	1.13	1.76	1.88	1.48	1.68	1.59	1.72	1.81
MgO	0.16	0.10	0.11	0.08	0.10	0.10	0.10	0.09	0.11	0.11	0.05	0.06	0.04	0.06	0.06	0.05
Total	99.98	100.07	100.30	100.27	100.18	100.02	100.07	100.00	99.77	99.97	99.52	100.13	97.72	100.20	100.49	99.80
Atoms per formula unit (based on three anions and two cations)																
Ti	0.008	0.010	0.012	0.012	0.022	0.020	0.027	0.029	0.028	0.041	0.042	0.034	0.037	0.037	0.039	0.041
Al	0.017	0.013	0.007	–	0.002	–	–	–	–	0.002	0.002	0.002	–	0.001	0.002	0.002
Cr	1.110	0.909	0.608	0.528	0.462	0.434	0.383	0.346	0.317	0.280	0.267	0.333	0.267	0.271	0.261	0.236
V	0.731	0.905	1.178	1.203	1.207	1.196	1.214	1.179	1.201	1.180	1.183	1.104	1.142	1.118	1.070	1.081
Fe^{3+}	0.126	0.155	0.184	0.244	0.283	0.330	0.349	0.417	0.426	0.456	0.464	0.494	0.516	0.537	0.590	0.599
Fe^{2+}	0.002	0.004	0.007	0.010	0.020	0.016	0.023	0.026	0.024	0.037	0.040	0.031	0.036	0.034	0.036	0.039
Mg	0.006	0.004	0.004	0.003	0.004	0.004	0.004	0.003	0.004	0.004	0.002	0.002	0.002	0.002	0.002	0.002
Total	2.000	2.000	2.000	2.000	2.000	2.000	2.000	2.000	2.000	2.000	2.000	2.000	2.000	2.000	2.000	2.000
Components, mol.%																
Karelianite	36.6	45.3	58.9	60.2	60.4	59.8	60.7	58.9	60.1	59.0	59.2	55.2	57.1	55.9	53.5	54.1
Eskolaite	55.5	45.5	30.4	26.4	23.1	21.7	19.2	17.3	15.9	14.0	13.4	16.7	13.4	13.6	13.1	11.8
Hematite	6.3	7.8	9.2	12.2	14.2	16.5	17.5	20.9	21.3	22.8	23.2	24.7	25.8	26.9	29.5	30.0
Others	1.6	1.4	1.5	1.2	2.3	2.0	2.6	2.9	2.7	4.2	4.2	3.4	3.7	3.6	3.9	4.1

Note. Fe_2O_3/FeO according to calculations. SiO_2, MgO, and ZnO are below detection limit (0.01–0.02 wt.%).

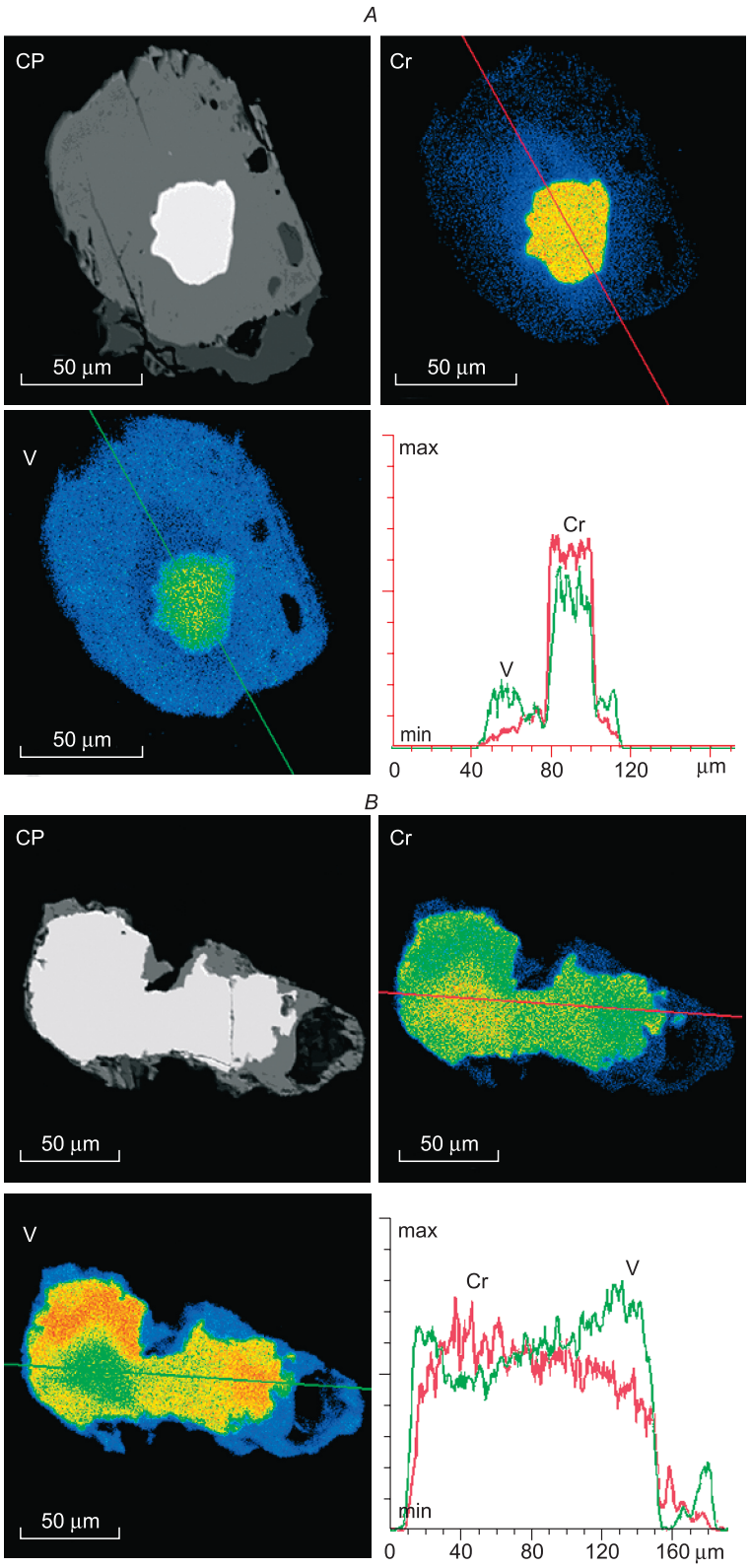

Fig. 6. Correlated distribution of Cr and V in diopside and karelianite–eskolaite inclusions. *A*, markedly decreasing Cr content in pyroxene; V is relatively high throughout the pyroxene grain and is slightly lower near a karelianite–eskolaite inclusion and in its margin; *B*, uneven distribution of Cr and V in the karelianite–eskolaite inclusion. BSE images (CP) and X-ray maps of Cr and V.

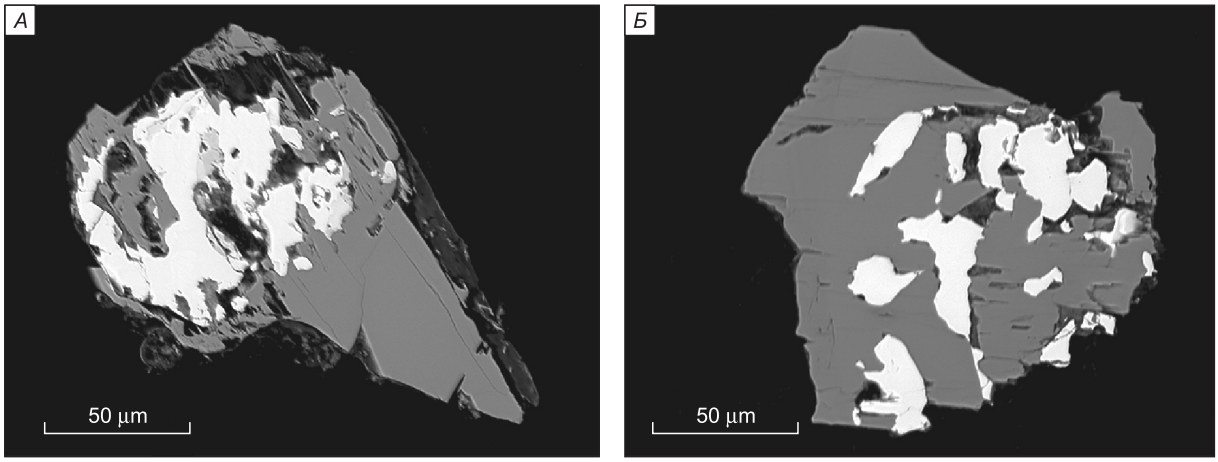

Fig. 7. Kosmochlor–natalyite pyroxene with a large partly resorbed inclusion (*A*) and numerous small karelianite–eskolaite inclusions (*B*).

anite–clinopyroxene equilibrium and for the "dissolution" of the oxide mineral in diopside and in most of Cr–V-bearing pyroxenes in general, with the formation of aureoles. The process often remained incomplete and the initial reaction products were preserved due to low rates of Cr and V diffusion. Primary euhedral karelianite–eskolaite remained mainly as "armored" inclusions in quartz. The heterogeneity of pyroxenes and karelianite–eskolaite inclusions results from two factors. First, V diffused more rapidly (Reznitsky et al., 1988) while the oxide phases and pyroxene differed in relative Cr–V affinity, with the Cr/V ratio always higher in the former, sometimes orders of magnitude (Fig. 13). Second, the diffusion rates possibly varied with crystallographic direction in minerals, which may account for frequently observed complex Cr and V patterns, especially, in relict eskolaite.

The presence of inclusions indicates that karelianite–eskolaite participated in the formation of Cr–V-bearing aluminosilicates (micas and tourmaline), which show isovalent substitutions $(V,Cr)^{3+} \rightarrow Al_{VI}$, unlike pyroxenes. This may be the reason why Cr and V are more often evenly distributed in aluminosilicates and in karelianite–eskolaite inclusions they host.

Genetic types of eskolaite and karelianite: natural occurrence vs. experimental data

Generally, there are several genetic types of eskolaite. Magmatic escolaite forms syngenetic inclusions in chromite from ultramafic rocks in the Polar Urals (Rai-Iz and Voikar-Syniya intrusions), where it coexists with PGE sulfides and other refractory minerals having crystallization temperatures no lower than 900–1000 °C (Moloshag et al., 1996, 1999; Yang et al., 2015). Eskolaite occurs along grain boundaries between Cr-bearing ilmenite and magnetite or as inclusions in magnetite from the Kusinsky gabbro intrusion that crystallized at the final stage from an ore-bearing melt (Bocharnikova and Voronina, 2008). Eskolaite coexisting with Cr-tourmaline and micas in the Bazhenov intrusion formed by metasomatism at the postmagmatic stage (Erokhin, 2006). Magmatic eskolaite is present also in meteorites: that in the Orgueil meteorite possibly crystallized together with magnesiochromite and kosmochlor (Greshake and Bischoff, 1996); in ureilite LEW88774, it occurs as microinclusions at boundaries with chromite in glass produced by decompression melting when its parent body rose to the surface (Prinz et al., 1994); eskolaite in the Martian Allan Hills meteorite formed by chromite decomposition during impact melting (Barber and Scott, 2006). Meteorites contain also eskolaites of other genetic types: eskolaite in carbonaceous chondrite may have condensed together with P-sulfides from the solar nebula at the protoplanetary stage (Nazarov et al., 2009); eskolaite found in the Martian Murchison CM chondrite along the margins of serpentinized chondrules in association with chromite and Cr-sulfides possibly resulted from oxidation when the temperature decreased to 600 °C (Ma et al., 2011); the origin of eskolaite in NWA 7533, another Martian meteorite, was attributed to hydrothermal processes in the Martian crust (Liu et al., 2016).

Genetically diverse eskolaites occur also in kimberlites. In the Udachnaya kimberlite (Yakutia), eskolaite was first found in mantle inclusions of grospydite and kyanite eclogite that formed at 20–30 kbar and 1200–1300 °C (Sobolev, 1974). Later eskolaite that presumably precipitated from a C–O–H-bearing fluid was found in the same pipe intergorwn with or enclosed in diamond (Logvinova et al., 2008). On the other hand, eskolaite in the Moses Rock kimberlite (USA), though occurring in mantle inclusions of omphacite pyroxenite, resulted from complex postmagmatic alteration of the host rock: metamorphism, metasomatism, as well as hydration and subsequent dehydration of guyanaite (a hydrous oxide) in a subduction setting at T 650–800 °C (Schulze et al., 2014). Relatively low-temperature hydrothermal kimberlite-hosted eskolaite, as a product of Cr-diopside decomposition, was reported from the White Sea region (So-

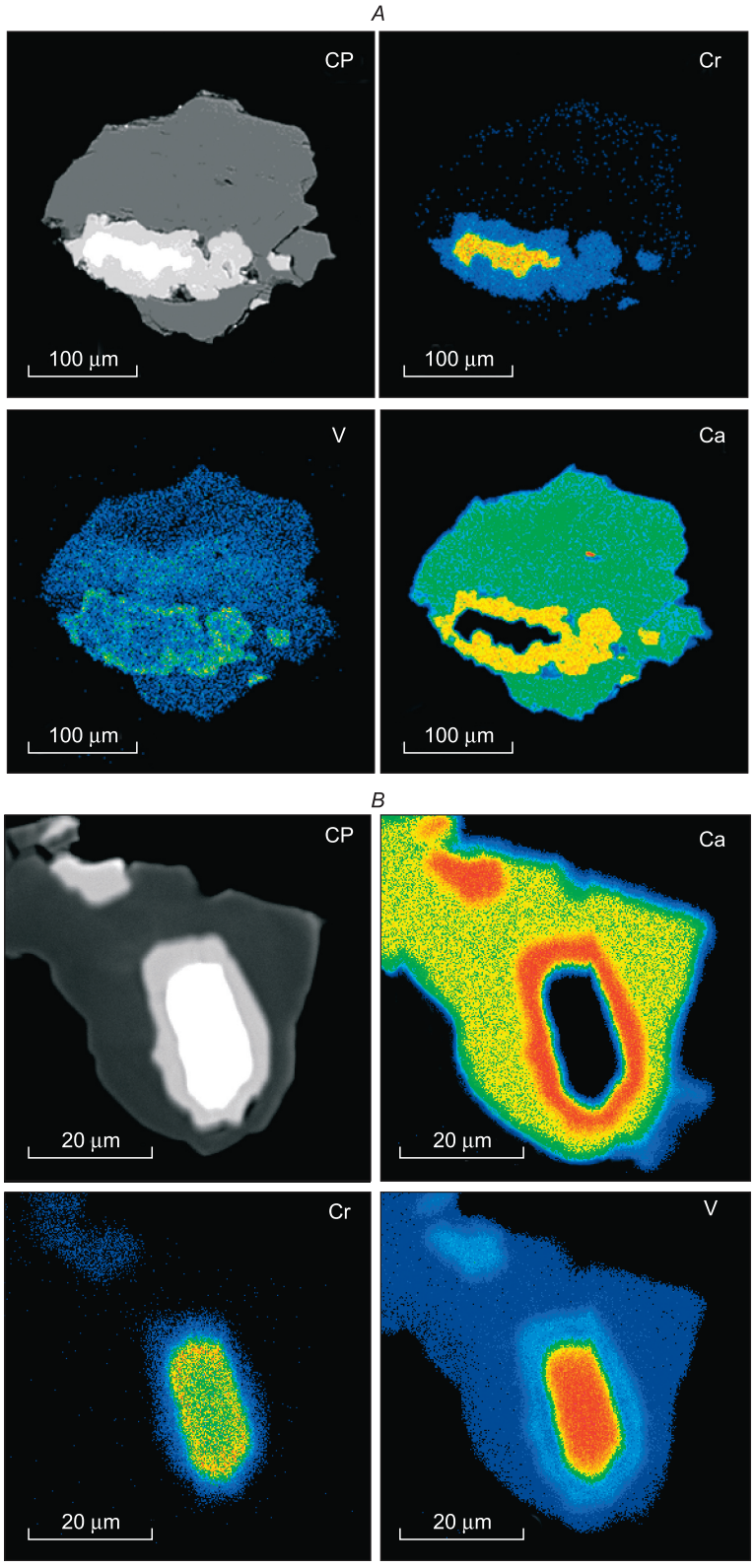

Fig. 8. Garnet margin around a karelianite–eskolaite inclusion in diopside (*A*) and epidote (*B*). BSE images (CP) and X-ray maps of Ca, Cr and V.

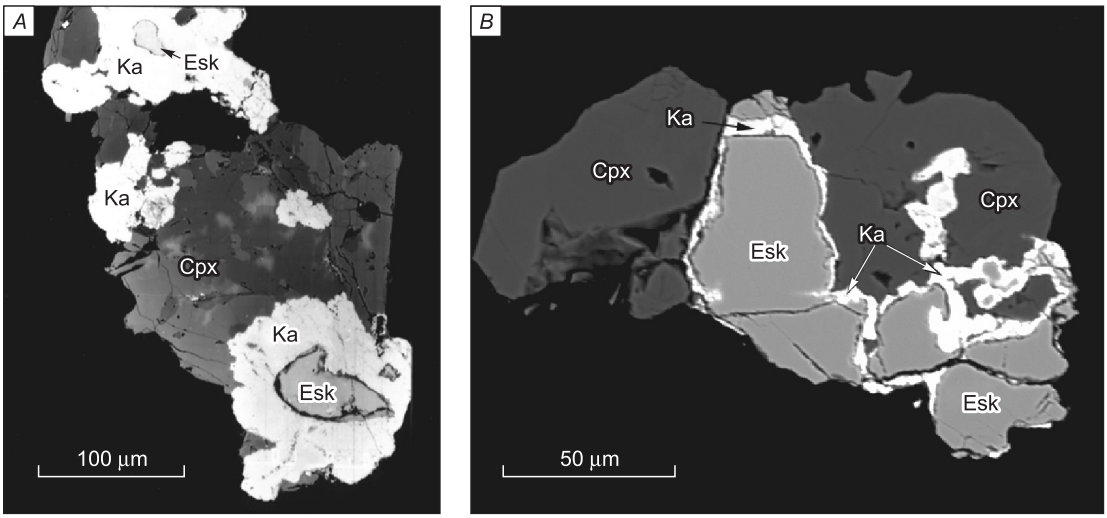

Fig. 9. Karelianite–eskolaite inclusions in kalininite–florensovite (*A*) and a sulfospinel margin around a karelianite–eskolaite inclusion in pyroxene (*B*). BSE image. Cpx, pyroxene; Ka, kalininite–florensovite; Esk, eskolaite–karelianite.

bolev et al., 1993). Similar origin was inferred for eskolaite coexisting with barite in siltstone around kimberlite pipes in the same region. Metamorphic eskolaite is known from the Baikal region and from a metamorphic graphite deposit in Dukou, Sichuan, China (Zhang et al., 1987). Eskolaite can form also in medium-temperature (500–600 °C) hydrothermal-metasomatic rocks: it is a major constituent in merumite, which is a complex assemblage of chromian minerals derived from hydrothermally altered ash and sandstone (Milton et al., 1976); eskolaite was also reported from Cr–V-bearing micaceous metasomatic rocks in the Onega basin in Karelia (Rumyantseva and Lapshin, 1986) and the Kosva Kamen carbonatite in the Urals (Ivanov and Philippov, 2012).

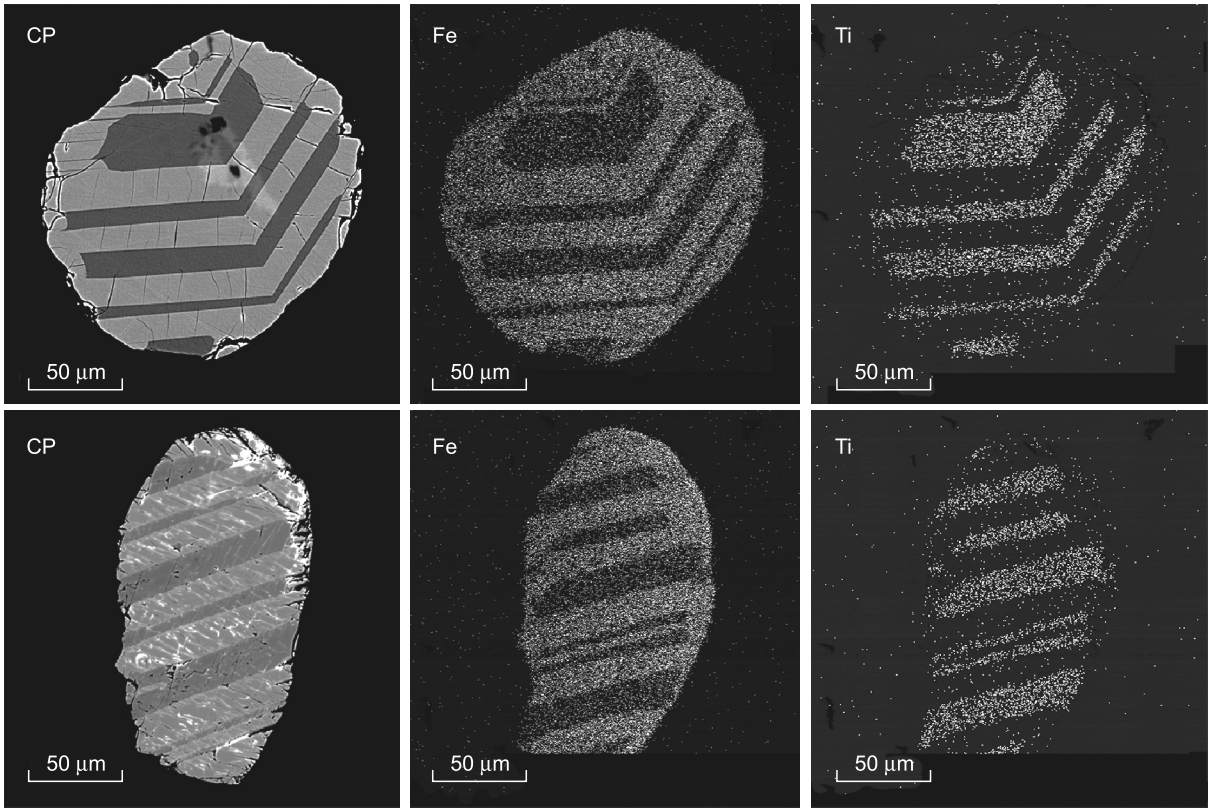

Fig. 10. Mixed crystals with layer-by-layer growth of Fe-karelianite and Ti-oxyvianite. BSE (CP) images and X-ray maps of Fe and Ti.

Karelianite differs markedly from eskolaite in occurrence. It is mainly found in low- to medium-temperature hydrothermal metasomatic deposits, such as the Outokumpu deposit; the Vihanti sulfide ore deposit in Finland (Sergeeva et al., 2011); medium-grade metamorphic sulfide ore of the Pyrrhotite Gorge deposit (Karpov et al., 2013); the Hemlo mesothermal Au deposit in Canada (Harris, 1989); and the Tuvati Au–Te–Ag deposit in Fiji (Spry and Scherbarth, 2006). Karelianite occurs also in low-temperature (150–200 °C) hydrothermal veins: calcite veins in the Onega Cr–V micaceous metasomatics (Rumyantseva and Lapshin, 1986) and in the Buca della Vena barite deposit in Italy (Orlandi and Checchi, 1986), as well as in quartz veins with sulfides in graphite gneiss of the Merelani Hills tanzanite deposit in Tanzania (Giuliani et al., 2008). Lowest-temperature karelianite in association with V hydroxides occurs in the Mounana sandstone-hosted U deposit in Gabon (Geffroy et al., 1964; Agrinier and Geffroy, 1969; Saint-Martin, 1977), the Urcal deposit in Argentina (Brodtkorb, 1982), and a deposit of vanadiferous anthraxolite bitumen from Guangxi in China (Liu and Lin, 1984).

Meanwhile, karelianite has been never found in igneous rocks; it is present in medium- and high-grade metamorphic rocks as part of the $(Cr,V)_2O_3$ ss series (see below), with the exception of the Green Giant deposit in Madagascar (Di Cecco et al., 2018) where it belongs to the assemblage of high-temperature gneiss together with other V- and V–Ti-oxides (provided that the mineral did form during prograde metamorphism).

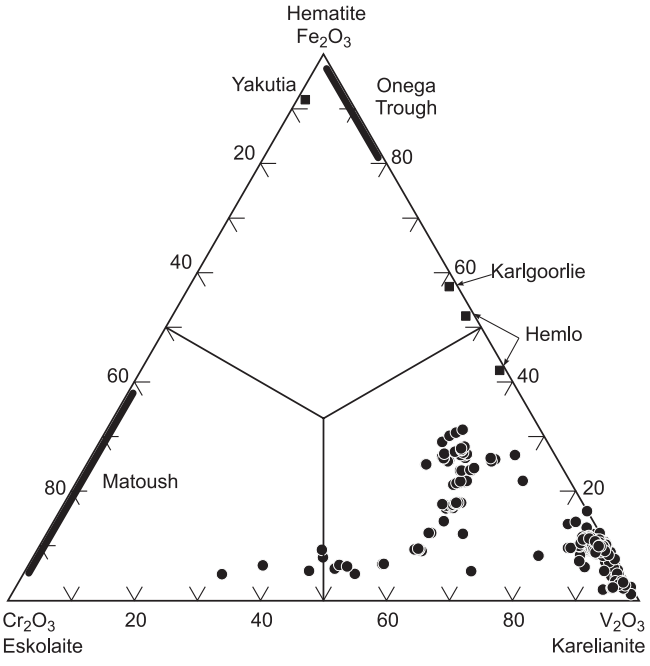

Fig. 11. Hematite–eskolaite–karelianite diagram for Fe-karelianites and three-component solid solutions (Cr, Fe, V)$_2O_3$ from the Slyudyanka rocks.

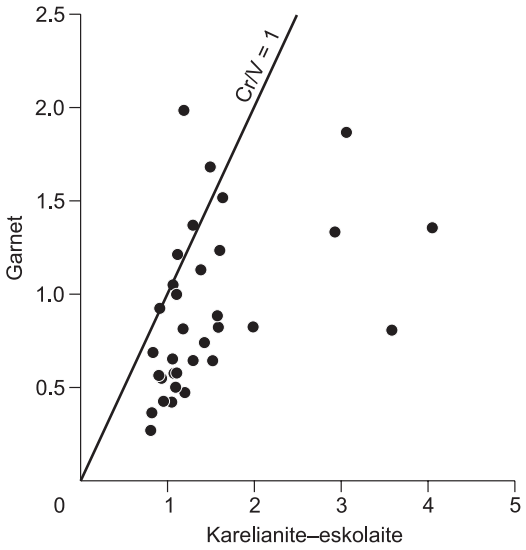

Fig. 12. Cr/V ratios in coexisting garnet and karelianite–eskolaite.

Experimental results, in principle, agree with the field data. Eskolaite crystals were grown from a melt by the Verneuil flame fusion at 1450 °C (Gendelev and Semenova, 1980); Cr_2O_3 crystallized at the same temperature when glass was obtained from ferrochromite slag in experiments reported by Dvornichenko and Shcheglova (1984). Like the naturally occurring escolaite, its synthetic analog was obtained by decomposition of chromite at 1000 °C or higher (Karyakin et al., 1956; Bozadzhiev, 1984) and by reaction of chromite with carbonated fluid at the mantle *PT*-conditions (Bataleva et al., 2002). The eskolaite mineral paragenesis formed in the same way at 28–60 kbar and 1000 °C during synthesis of pyrope-knorringite garnets (Doroshev et al., 1997; Girnis et al., 2003). Eskolaite was also synthesized by a laser-induced vapor-phase reaction (Oyama et al., 1998, 1999). Finally, it appeared in association with magnesiochromite and kosmochlor during hydrothermal synthesis of the latter at 500–700 °C (Yoder and Kullerud, 1971; Vredevoogd and Forbes, 1975).

V_2O_3 was often synthesized by reduction of oxide or other V^{5+} compounds in a hydrogen medium at 900–1000 to 500–600 °C (Cox et al., 1962; Ruan and Cui, 1997; Chudnovskii et al., 1998; Xu et al., 2008; etc.). Experiments of recent decades have led to synthesis of micro- and nanometer karelianite crystals with strong photocatalytical properties. In other experiments, karelianite was synthesized from V_2O_5, hydroxides and complex compounds of vanadium doped with other, mainly organic, solutions, at 350 to 220 °C. The crystallization temperature depended on the starting mixture composition and run duration, and was as low as 200 °C in some runs (Blagojevic et al., 2010; Ishiwata et al., 2012; Bai et al., 2013; Zdravkov et al., 2016; etc.). Note that eskolaite was never synthesized at such low temperatures.

Generally, karelianite and eskolaite record the formation temperatures of their host rocks and can be used for refer-

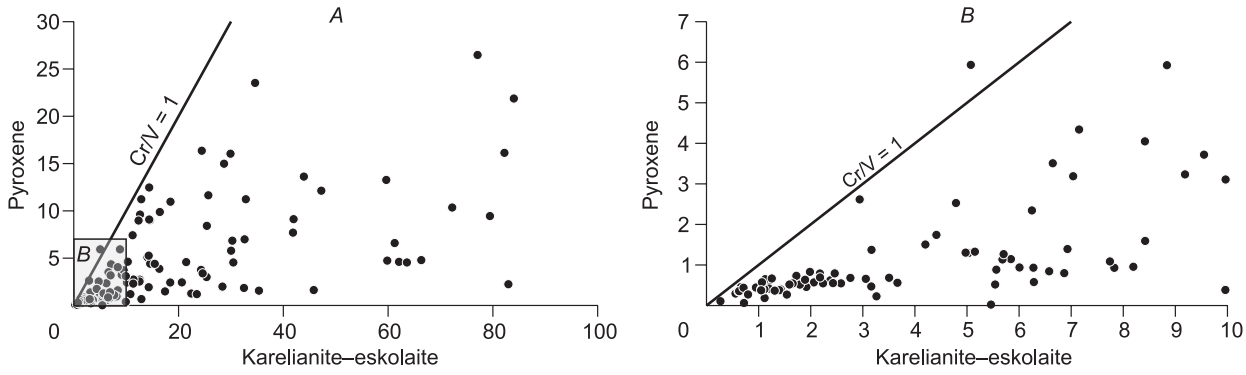

Fig. 13. Cr/V ratios in coexisting clinopyroxene and karelianite–eskolaite.

ence. This is, for instance, the case of a Cr and V deposit in the Onega basin where eskolaite is present in micaceous metasomatic rocks while karelianite coexists with montroseite in later low-temperature calcite veins (Rumyantseva and Lapshin, 1986).

V_2O_3–Cr_2O_3–Fe_2O_3–Al_2O_3 solid solutions: natural occurrence and synthesis

Cr_2O_3–V_2O_3 solid solution was synthesized from a mixture of oxides, most often at temperatures >1000 °C or in some cases up to 1200–1450 °C (Reid et al., 1972; Chudnovskii et al., 1998; etc.). Nanometer particles of $(Cr,V)_2O_3$ double oxide were obtained at high temperatures by a vapor-phase explosive reaction of a CrO_2Cl_2 + $VOCl_3$ + H_2 + O_2 gas mixture irradiated with a pulsed laser (Oyama et al., 1998, 1999). Note that the critical temperature of the Cr_2O_3–V_2O_3 system solvus, at equal shares of Cr and V, is 895 °C, according to thermodynamic calculations based on experimental data (Kim and Sanders, 2001).

Continuous Cr_2O_3–V_2O_3 ss series is known from two more natural occurrences besides the Olkhon and Slyudyanka complexes: the high-grade metamorphic stratiform Rampura Agucha Pb–Zn–Ag deposit in India (Hoeller and Stumpfl, 1995) and the Namalulu tsavorite deposit in gneiss and marble (Feneyrol et al., 2012). Karelianite in the two deposits occurs as exsolution lamelli in chromite (Rampura Agucha) or in lenses of siliceous-carbonate rocks (Namalulu) and contains 18 to 41 wt.% and 24 to 35 wt.% Cr_2O_3, respectively. Meanwhile, thermodynamic calculations (Kim and Sanders, 2001) predict a narrower $(Cr,V)_2O_3$ miscibility gap at 20–25 mol.% Cr_2O_3 in V_2O_3 and V_2O_3 in Cr_2O_3 at the temperatures of amphibolite and granulite facies (~700–800 °C). Thus, the compositions of natural minerals transcend the gap and disagree with experimental and theoretical results.

An almost complete *V_2O_3–Fe_2O_3* ss series of $(V,Fe)_2O_3$ was synthesized from a mixture of oxides at ≥1000 °C (Cox et al., 1962) or at lower temperatures by mechanochemical activation (Sorescu et al., 2013); in the latter case, the temperature depended on the time of activation (size reduction to nanometer particles). Natural karelianite is a ferrophobic mineral, commonly with 0.*n* to a few wt.% Fe_2O_3, even though it frequently occurs in association with iron sulfide. Rare cases of high Fe enrichment in karelianite are known from the Pyrrhotite Gorge deposit with 7–8 wt.% Fe_2O_3 (Karpov et al., 2013). Oxides of unique composition $(V, Fe)_2O_3$ were found at the Hemlo gold deposit (Harris, 1989) where zoned crystals have hematite cores of 40.6 wt.% V_2O_3 and karelianite rims with exceptionally high Fe_2O_3 reaching 38.3 wt.%. The Hemlo deposit was formed hydrothermally at medium temperatures (400–500 °C), while Au together with V presumably were remobilized during late hydrothermal alteration at low temperatures (Pan and Fleet, 1992). Therefore, the mineral chemistry is inconsistent with the temperatures of $(V,Fe)_2O_3$ synthesis. Hematite with 39.6 wt.% V_2O_3 from the Au–Te Kalgoorlie deposit in Australia (Nickel and Grey, 1982) is another example of such an anomaly. Commonly V-hematite is of more frequent occurrence than Fe-karelianite. It forms veinlets and pseudomorphs after nolanite, karelianite, and roscoelite in Cr–V-bearing micaceous and carbonate-micaceous metasomatic rocks of the Onega basin, and its V_2O_3 contents vary from 0.*n* to 13.75 wt.% in different generations (Ryzhov et al., 1991). The V_2O_3 content in hematite from deep oxidation zones of U–V deposits in the same region is within 10.6 wt.% (Chernikov et al., 2005).

Cr_2O_3–Fe_2O_3 solid solutions were synthesized many times by different methods, which often led to discordant results. A complete $(Cr,Fe)_2O_3$ ss series formed at 950–1000 to 1200 °C or higher (Busca et al., 1993; Musić et al., 1993, 1996; Grygar et al., 1999; and many others). The available experimental data are presented in reviews of Grygar et al. (2003) and Murakami et al (2003) who discuss their own and published experiments. They show that the existence of a miscibility gap above 700 °C, and more so at >1000–1100 °C, is doubtful and is an erroneous inference based on synthesis by unsuitable techniques (Grygar et al., 2003). In the other paper (Murakami et al., 2003), the phase diagram with a critical temperature of 935 °C is interpreted as corresponding to metastable phase relation because the results depend strongly on run duration. However, high-tempera-

ture synthesis (at 1350–1650 °C) yielded eskolaite containing 5.4 to 7.2 wt.% Fe_2O_3, i.e., far from saturation; note that Cr and Fe came from chromite in the precursor composition and from ferromagnesite in the forming mineral assemblage (Bataleva et al., 2012).

Natural eskolaite is ferrophobic, like karelianite, with commonly 0.*n* to a few wt.% Fe_2O_3, and is often associated with chromite in high-temperature rocks (chromitite, meteorite, granulite) and even magnetite (Dukou metamorphic deposit and NWA 7533 meteorite). There are a few exceptions though. One analysis of eskolaite from the Kusinsky magnetite-ilmenite ores showed 16.24 wt.% Fe_2O_3, but some Fe input may be due to capture of Fe-phases by the beam because the eskolaite particles are very fine. Eskolaite from the Moses Rock kimberlite contains 8.19 wt.% Fe_2O_3, but it formed by dehydration of high-Fe guyanaite (Cr,Fe)O(OH). The highest Fe_2O_3 up to 36.6 wt.% was measured in eskolaite at the Matoush uranium deposit in Canada (Alexandre et al., 2014) located at the margin of a porphyritic mafic dike that intruded sandstones of the Otish Basin. The authors do not give explicit temperature estimates but note that eskolaite and uraninite crystallized late during the hydrothermal process, after Cr-micas and tourmaline, i.e., at relatively low temperatures. Hematite with 7.14 wt.% Cr_2O_3 was also reported from a kimberlite dike in Yakutia (Oleinikov, 1998).

The *Cr_2O_3–Al_2O_3* system has had controversial interpretations. In an early publication on synthesis of a complete series of solid solutions (Chatterjee et al., 1982), the critical temperature was estimated to be about 970–975 °C, while a later estimate (Roy and Barks, 1972), for P_{H_2O} from 1 bar to 50 kbar, gave a range from 945 to 989 °C. In the latter case, the pressure-dependent temperature gradient was only 0.8 °C per 1 kbar, and the solid solution Cr_2O_3–Al_2O_3 was recommended as a good geothermometer. The experiments and thermodynamic models reported by Kim and Sanders (2001) led to large deviation of the critical temperature from the top of the solvus curve which is highly asymmetric: the system attains complete miscibility only at 1271 °C and X_{Cr} = 0.3. However, synthesis in the MgO–Al_2O_3–SiO_2–Cr_2O_3 system at mantle *PT* conditions by Girnis et al. (2003) yielded eskolaite in association with corundum at a critical temperature of 890 °C and X_{Cr} = 0.48, i.e., close to the results of Chatterjee et al. (1982).

There is a sole natural occurrence of Al-eskolaite in association with Cr-corundum (Sobolev, 1974) which form inclusions or integrowths with Cr-kyanite in grospydite and kyanite eclogite from the Udachnaya kimberlite. Corundum contains up to 40.7 wt.% Cr_2O_3 or ~33 mol.% eskolaite, while eskolaite bears 26.3 wt.% Al_2O_3 or 37 mol.% of the corundum component. These very values were used (Chatterjee et al., 1982) to illustrate the applicability of the $(Cr,Al)_2O_3$ solid solution as a geothermometer. Al-eskolaite with up to 20–26 wt.% Al_2O_3 was also found in ureilite LEW 88774, where the coexisting glass encloses corundum microcrystals. Thus, Al-eskolaite has its natural occurrence limited to these two cases, where it coexists with corundum. Elsewhere, eskolaite contains no more than 0.*n*–a few wt.% Al_2O_3, even if it coexists with Al-minerals (kyanite and sillimanite) in high-temperature rocks. For instance, Al_2O_3 is within 5.5 wt.% in eskolaite from the Olkhon high-temperature gneiss with Cr-bearing kyanite (Koneva and Suvorova, 1995; Koneva, 2002), though eskolaite can accommodate 20–25 mol.% of the corundum component at 700–800 °C, according to different experimental measurements and calculations.

The notable discordance of experimental results with one another and with thermodynamic calculations may result from the lack of equilibrium between run products (slow ion diffusivity, short run durations), problems of preparing homogeneous precursor material of a known composition, as well as inhomogeneity of the charge and the synthesized phases; some of the causes are also relevant to natural solid solutions. However, the main reason is the dissimilarity of synthesis techniques, especially, as to starting mixture preparation and composition. The precursor mixtures are often made by codissolution of hydrosalts and Cr, V, Al, and Fe hydroxides or their gel mixtures, with subsequent stepwise synthesis, and the results differ markedly from those obtained with a mixture of oxides. The phase composition of the charge also matters, as it was proven experimentally by Girnis et al. (2003), who reanalyzed the earlier experiments of Doroshev et al. (1977). The Al contents in the synthesized eskolaite differed depending on the presence of corundum, at the same bulk chemistry of the charge.

The results of the above synopsis of synthesis experiments with solid solutions lead to some inferences concerning natural minerals.

The presence of large-range eskolaite–karelianite ss series in rocks indicates quite high formation temperatures (at least 600–700 °C), though does not allow quantitative evaluation because the results of different experimental studies disagree with one another and with data on natural minerals. High Fe contents in karelianite and eskolaite cannot be a *PT* proxy but rather provide evidence of special geochemical conditions of petrogenesis as to the protoliths and/or fluids. Anyway, the Slyudyanka ferrian eskolaite–karelianite formed only in rocks that differed from the general series of Cr–V-bearing rocks in chemistry and paragenesis. The unusual high-Fe compositions of karelianite–hematite from the Hemlo and Kalgoorlie deposits and eskolaite from the Matoush deposit remain poorly understood.

Aluminum can be used as a geothermometer only in the case of escolaite–corundum paragenesis. Even the initial presence of corundum in the protolith does not guarantee that Al content in eskolaite would be a reliable temperature tracer. Aluminum in eskolaite synthesized at the mantle *PT* parameters from a charge containing Al_2O_3 (Bataleva et al., 2012) was no more than 10.8 wt.%, or much below the saturation the mineral could reach at 1350 °C and 15% Al_2O_3 in the charge.

Another feature of karelianite and eskolaite, which often remains overlooked, is their frequent association with sul-

fides, especially, with pyrrhotite (of course, not including sulfide ores proper). It was mentioned in many of the publications cited above: eskolaite coexisting with pyrite and pyrrhotite in the Alan Hills meteorite and with chromite in Murchison is localized around inclusions of murchisite (Cr_5S_6) in serpentine; karelianite forms rims around rutile enclosed in pyrrhotite in hornfelsed xenolith from the Khibiny alkaline intrusion and occurs at contacts with pyrrhotite at the Merelani-Hills and Green Giant deposits. The relation of eskolaite with sulfides, including in chromitite, has received genetic interpretation (Ivanov and Philippov, 2012) only for the case of the Kosva Kamen carbonatite intrusion margins, where lath-like eskolaite surrounds Cr-bearing pyrite that replaces chromite and, in its turn, is overgrown with kalininite (sufospinel). Ivanov and Philippov (2012) explain the eskolaite–sulfide association in the context of chromite sulfidization leading to the "disposal" of oxygen-loving Cr into eskolaite. The Slyudyanka eskolaite overgrown with kalininite–florensovite resembles this situation, but in the absence of chromite.

CONCLUSIONS

The continuous karelianite–eskolaite join in Cr–V-bearing rocks of the Slyudyanka metamorphic complex formed during regional prograde metamorphism and made basis for crystallization of Cr–V-bearing and Cr–V minerals in the complex.

In a general case, karelianite and eskolaite have different crystallization temperatures and can be used for reference as indicators of formation temperatures of their hosts. The karelianite–eskolaite solid solutions containing >15–20 mol.% of one component indicate crystallization at no lower than 600–700 °C.

The escolaite-karelianit-hematite solid solutions do not record the *PT* parameters of crystallization but rather provide evidence of specific geochemical conditions of petrogenesis. Isomorphic admixture of Al in eskolaite in paragenesis with corundum may be used as a geothermometer.

REFERENCES

Agrinier, H., Geffroy, J., 1969. Microscopic iconography of some minerals from uraniferous deposits in France and Gabun. Bull. Inform. Sci. Tech. (Paris) 137, 77–81.

Alexandre, P., Peterson, R.C., Kyser, K., Layton-Matthews, D., Joy, B., 2014. High-Cr minerals from the Matoush uranium deposit in the Otish Basin, Quebec, Canada. Can. Mineral. 52 (1), 61–75.

Bai, Y., Jin, P., Ji, S., Luo, H., Gao, Y., 2013. Preparation and characterization of V_2O_3 micro-crystals via a one-step hydrothermal process. Ceram. Int. 39 (7), 7803–7808.

Barber, D.J., Scott, E.R.D., 2006. Shock and thermal history of Martian meteorite Allan Hills 84001 from transmission electron microscopy. Meteorit. Planet. Sci. 41 (4), 643–662.

Bataleva, Yu.V., Pal'yanov, Yu.N., Sokol, A.G., Borzdov, Yu.M., Sobolev, N.V., 2012. Conditions of formation of Cr-pyrope and escolaite during mantle metasomatism: Experimental modeling. Dokl. Earth Sci. 442 (1), 76–80.

Blagojevic, V.A., Carlo, J.P., Brus, L.E., Steigerwald, M.L., Uemura, Y.J., Billinge, S.J.L., Zhou, W., Stephens, P.W., Aczel, A.A., Luke, G.M., 2010. Magnetic phase transition in V_2O_3 nanocrystals. Phys. Rev. B. 82, 094453.

Bocharnikova, T.D., Voronina, L.K., 2008. The first finding of eskolaite in magnetite-ilmenite ores of the Kusinsky gabbro intrusion, in: Bulletin–2007 (Trans. IGG UrO RAN, Issue 155) [in Russian]. Yekaterinburg, pp. 226–229.

Bogatikov, O.A., Gorshkov, A.I., Mokhov, A.V., Ashikhmina, N.A., Sivtsov, A.V., 2001. Cadmium-bearing wurtzite and eskolaite: new ore minerals in the Luna 24 regolith. Dokl. Earth Sci. 379A (6), Part 2, 679–681.

Bozadzhiev, L., 1984. X-ray diffraction analysis of thermally treated chromite. God. VUZ. Tekhn. Fiz. 20 (1), 191–196.

Busca, G., Ramis, G., del Carmen Prieto, M., Escribano, V.S., 1993. Preparation and characterization of $Fe_{2-x}Cr_xO_3$ mixed oxide powders. J. Mater. Chem. 3 (6), 665–673.

Cassedanne, Ja., Cassedanne, Je., 1980. Présence d'eskolaite dans les alluvions stannifères de la Chapada Diamantina (Bahia-Brésil). Bull. Mineral. 103, 600–602.

Chatterjee, N.D., Leistner, H., Terhart, L., Abraham, K., Klaska, R., 1982. Thermodynamic mixing properties of corundum-eskolaite, α-$(Al,Cr^{3+})_2O_3$, crystalline solid solutions at high temperatures and pressures. Am. Mineral. 67, 725–735.

Chernikov, A.A., Dubinchuk, V.T., Chistyakova, N.I., Naumova, I.S., Zaitsev, V.S., 2005. New data on V hematite, micro- and nanometer crystals of related minerals of noble metals, Cu, Zn, and Fe. Novye Dannye o Mineralakh 40, 65–71.

Chudnovskii, F.A., Pergament, A.L., Stefanovich, G.B., Metcalf, P.A., Honig, J.M., 1998. Switching phenomena in chromium-doped vanadium sesquioxide. J. App. Phys. 84 (5), 2643–2646.

Cox, D.E., Taxei, W.J., Miller, R.C., Shirane, O., 1962. A magnetic and neutron diffraction study of the Fe_2O_3–V_2O_3, system. J. Phys. Chem. Solids 23, 863–874.

de Brodtkorb, M.K., 1982. Vanadium oxides in the Urcal deposit, Argentina, in: Amstutz, G.C. El Goresy, A., Frenzel, G., Kluth, C., Moh, G., Wauschkuhn, A., Zimmermann, R.A. (Eds.), Ore Genesis. The State of the Art. Special Publication of the Society for Geology Applied to Mineral Deposits, Vol. 2. Springer, Heidelberg, Berlin, pp. 221–229.

Di Cecco, V.E., Tait, K.T., Spooner, E.T.C., Scherba, C., 2018. The vanadium-bearing oxide minerals of the Green Giant vanadium-graphite deposit, Southwest Madagascar. Can. Mineral. 56 (3), 247–257.

Doroshev, A.M., Brey, G.P., Girnis, A.V., Turkin, A.I., Kogarko, L.N., 1997. Pyrope-knorringite garnets in the Earth's mantle: experiments in the MgO–Al_2O_3–SiO_2–Cr_2O_3 system. Geologiya i Geofizika (Russian Geology and Geophysics) 38 (2), 523–545 (559–586).

Dvornichenko, I.N., Shcheglova, M.D., 1984. Mineral inclusions in slag Cr aventurine glass. Izv. AN SSSR. Neorganicheskie Materialy 20 (10), 1730–1732.

Erokhin, Yu.V., 2006. Chromite mineralization of the Bazhenov ophiolite suite (Central Urals). Litosfera 3, 160–165.

Feneyrol, J., Ohnenstetter, D., Giuliani, G., Fallick, A.E., Rollion-Bard, C., Robert, J.-L., Malisa, E.P., 2012. Evidence of evaporites in the genesis of the vanadian grossular "tsavorite" deposit in Namalulu, Tanzania. Can. Mineral. 50 (3), 745–769.

Geffroy, J., Cesbron, F., Lafforgue, P., 1964. Données préliminaires sur les constituants profonds des minerais uranifères et vanadifères de Mounana (Gabon). CR Acad. Sci. Paris II (259), 601–603.

Gendelev, S.Sh., Semenova, N.N., 1980. Morphology of synthetic eskolaite crystals. Zapiski VMO, No. 2, 246–248.

Girnis, A.V., Brey, G.P., Doroshev, A.M., Turkin, A.I., Simon, N., 2003. The system MgO–Al_2O_3–Cr_2O_3 revisited: reanalysis of Doroshev et al.'s (1997) experiments and new experiments. Eur. J. Mineral. 15 (6), 953–964.

Giuliani, G., Ohnenstetter, D., Palhol, F., Feneyrol, J., Boutroy, E., De Boissezon, H., Lhomme, Th., 2008. Karelianite and vanadian phlogopite from the Merelani Hills gem zoisite deposits, Tanzania. Can. Mineral. 46 (5), 1183–1194.

Greshake, A., Bischoff, A., 1996. Chromium-bearing phases in Orgueil (CI): discovery of magnesiochromite ($MgCr_2O_4$), ureyite ($NaCrSi_2O_6$), and chromium oxide (Cr_2O_3), in: 27th Lunar Planet. Sci. Conf., pp. 461–462.

Grygar, T., Bezdička, P., Caspary, E-G., 1999. Electrochemical dissolution of immobilized α-$(Fe_xCr_{1-x})_2O_3$ microparticles. J. Electrochem. Soc. 146 (9), 3234–3237.

Grygar, T., Bezdička, P., Dědeček, J., Petrovský, E., Schneeweiss, O., 2003. Fe_2O_3–Cr_2O_3 system revised. Ceram.–Silikaty 47 (1), 32–39.

Harris, D.C., 1989. The Mineralogy and Geochemistry of the Hemlo Gold Deposit, Ontario. Geological Survey of Canada, Econ. Geol. Rep. 38.

Hoeller, W., Stumpfl, E.F., 1995. Cr–V oxides from the Rampura Agucha Pb–Zn–(Ag) deposit, Rajasthan, India. Can. Mineral. 33 (4), 745–752.

Ishiwata, Y., Suehiro, S., Kida, T., Ishii, H., Tezuka, Y., Oosato, H., Watanabe, E., Tsuya, D., Inagaki, Y., Kawae, T., Nantoh, M., Ishibashi, K., 2012. Spontaneous uniaxial strain and disappearance of the metal-insulator transition in monodisperse V_2O_3 nanocrystals. Phys. Rev. B. 86, 035449.

Ivanov, O.K., Philippov, V.N., 2012. Kalininite—$ZnCr_2S_4$ and escolaite from intrusion contact of the Kosva Kamen' carbonatite in the Urals. Uralskii Geologicheskii Zhurnal 87 (3), 43–48.

Karpenko, V.Yu., Tishchenko, A.I., 1992. Finding of escolaite in silty sandstone of the Urzug Fm. in the Northwestern White Sea region. Mineralogicheskii Zhurnal 14 (1), 93–96.

Karpov, S.M., Voloshin, A.V., Savchenko, E.E., Selivanova, E.A., 2013. Vanadium minerals in ores of the Pyrrhotite Gorge pyrite deposit (Khibiny, Kola Peninsula). Zapiski RMO 3, 83–89.

Karyakin, L.I., Pyatikop, P.D., Sukharevskii, B.Ya., 1956. Alteration and interaction of Cr spinel with magnesioferrite upon heating. Dokl. AN SSSR 109 (5), 1009–1011.

Kim, S.S., Sanders, T.H., 2001. Thermodynamic modeling of the isomorphous phase diagrams in the Al_2O_3–Cr_2O_3 and V_2O_3–Cr_2O_3 systems. J. Am. Ceram. Soc. 84 (8), 1881–1884.

Kimura, M., Ikeda, Y., 1992. Mineralogy and petrology of an unusual Belgica-7904 carbonaceous chondrite: genetic relationships among the components. Proc. NIPR Symp. Antarct. Meteorites 5, 74–119.

Konev, A.A., Reznitsky, L.Z., Feoktistov, G.D., Sapozhnikov, A.N., Koneva, A.A., Sklyarov, E.V., Vorobiev, E.I., Ivanov, V.G., Ushchapovskaya, Z.F., 2001. Mineralogy of East Siberia at the Turn of the 21st Century (New and Rare Minerals) [in Russian]. Intermet Engineering, Moscow.

Koneva, A.A., 2002. Cr–V oxides in metamorphic rocks, Lake Baikal, Russia. N. Jb. Miner. Mh. 12, 541–550.

Koneva, A.A., Suvorova, L.F., 1995. Rare Cr and V oxides in metamorphic rocks of the Ol'khon region (Western Baikal area). Zapiski VMO 124 (4), 52–61.

Kouvo, O., Vuorelainen, Y., 1958. Eskolaite, a new chromium mineral. Am. Mineral. 43 (11–12), 1098–1106.

Liu, D., Lin, M., 1984. Discovery of some vanadium and nickel minerals from anthraxolite and discussion of their origin. Scientia Sinica, Series B 27 (11), 1197–1202.

Liu, Y., Ma, C., Beckett, J., Flannery, D., Allwood, A., 2016. Metamorphism on Mars: a view from eskolaite-bearing chromite-magnetites in Northwest Africa (NWA) 7533, in: 47th Lunar Planet. Sci. Conf., Abstr. 1127.

Long, J.V.P., 1963. Karelianite, a new vanadium mineral. Am. Mineral. 48 (1–2), 33–41.

Logvinova, A.M., Wirth, R., Sobolev, N.V., Seryotkin, Y.V., Yefimova, E.S., Floss, C., Taylor, L.A., 2008. Eskolaite associated with diamond from the Udachnaya kimberlite pipe, Yakutia, Russia. Am. Mineral. 93 (4), 685–690.

Ma, C., Beckett, J.R., Rossman, G.R., 2011. Murchisite, Cr_5S_6, a new mineral from the Murchison meteorite. Am. Mineral. 96 (11–12), 1905–1908.

Mikhailova, Yu.A., Konopleva, N.G., Yakovenchuk, V.N., Ivanyuk, G. Yu., Menshikov, Yu.P., Pakhomovsky, Ya.A., 2006. Corundum-group minerals in rocks of the Khibiny alkaline complex (Kola Peninsula). Zapiski RMO 6, 41–54.

Milton, C., Appleman, D.E., Appleman, M.H., Chao, E.C.T., Cuttitta, F., Dinnin, J.I., Dwornik, E.J., Ingram, B.L., Rose, H.J., Jr., 1976. Merumite, a Complex Assemblage of Chromium Minerals from Guyana. U.S. Geol. Surv. Prof. Pap. 887.

Mokhov, A.V., Kartashov, P.M., Bogatikov, O.A., 2007. The Moon under Microscope (New Data on Moon Mineralogy) [in Russian]. Nauka, Moscow.

Mokhov, A.V., Rybchuk, A.P., Kartashov, P.M., Gornostaeva, T.A., Bogatikov, O.A., 2017. Eskolaite in the regolith of the Taurus-Littrow Valley. Dokl. Earth Sci. 475 (2), 923–925.

Moloshag, V.P., Alimov, V.Yu., Vakhrusheva, N.V., Gulyaeva, T.Ya., 1996. The first finding of eskolaite in chromite ores of the Urals, in: Bulletin-1995 (Trans. IGG UrO RAN) [in Russian]. Yekaterinburg, pp. 147–148.

Moloshag, V.P., Alimov, V.Yu., Anikina, E.V., Gulyaeva, T.Ya., Vakkhrusheva, N.V., Smirnov, S.V., 1999. Accessory mineralization of chromitite in alpine-type ultramafics of the Urals. Zapiski VMO 2, 71–83.

Murakami, Y., Sawata, A., Tsuru, Y., Akiyama, K., 2003. Metastable phase relation and phase equilibria in the Cr_2O_3–Fe_2O_3 system. J. Mater. Sci. 38, 2723–2725.

Musić, S., Popović, S., Ristić, M., 1993. Chemical and structural properties of the system Fe_2O_3–Cr_2O_3. J. Mater. Sci. 28 (3), 632–638.

Musić, S., Lenglet, M., Popović, S., Hannoyer, B., Czakó-Nagy, I., Ristić, M., Balzar, D., Gashi, F., 1996. Formation and characterization of the solid solutions $(Cr_xFe_{1-x})_2O_3$, $0 \le x \le 1$. J. Mater. Sci. 31 (15), 4067–4076.

Nazarov, M.A., Kurat, G., Brandstaetter, F., Ntaflos, T., Chaussidon, M., Hoppe, P., 2009. Phosphorus-bearing sulfides and their associations in CM chondrites. Petrology 17 (2), 101–123.

Nickel, E.H., Grey, I.E., 1982. A vanadium-rich mineral assemblage associated with the gold telluride ores at Kalgoorlie, in: Proc. XIII Gen. Meet. (Varna, Bulgaria). Int. Mineral. Assoc., pp. 1–16.

Oleinikov, O.B., 1998. Deep metasomatic assemblages in intrusive kimberlite. Otechestvennaya Geologiya 6, 51–54.

Oppenheim, M.J., Brück, P.M., Elsdon, R., Synge F.M., Weaver, A., Warren, W.P., 1977. Eskolaite, Cr_2O_3, from County Wicklow, Ireland. Mineral. Mag. 41, 402–403.

Orlandi, P., Checchi, F., 1986. The Buca della Vena Mine, Tuscany, Italy. Mineral. Record 17 (4), 261–268.

Oyama, T., Iimura, Y., Takeuchi, K., Ishii, T., 1998. Vapor-phase synthesis of fine particles of Cr–V double oxide using a pulsed laser. J. Mater. Sci. Lett. 17 (20), 1751–1754.

Oyama, T., Iimura, Y., Takeuchi, K., Ishii, T., 1999. Synthesis of $(Cr_xV_{1-x})_2O_3$ fine particles by a laser-induced vapor-phase reaction and their crystal structure. J. Mater. Sci. 34 (3), 439–444.

Pan, Y., Fleet, M.E., 1992. Mineral chemistry and geochemistry of vanadian silicates in the Hemlo gold deposit, Ontario, Canada. Contrib. Mineral. Petrol. 109 (4), 511–525.

Prinz, M., Weisberg, M.K., Nehru, C.E., 1994. LEW 88774: a new type of Cr-rich ureilite, in: 25th Lunar Planet. Sci. Conf., pp. 1107–1108.

Ramdohr, P., 1977. Some observations in meteoritic microscopy as a suggestion for further research. Chem. Erde 36 (4), 263–286.

Reid, A.F., Sabine, T.M., Wheeler, D.A., 1972. Neutron diffraction and other studies of magnetic ordering in phases based on Cr_2O_3, V_2O_3 and Ti_2O_3. J. Solid State Chem. 4 (3), 400–409.

Reznitsky, L.Z., Sklyarov, E.V., Ushchapovskaya, Z.F., 1988. Cr and V minerals in the Slyudyanka metamorphic complex (Southern Baikal region), in: Precambrian Metamorphic Rocks in East Siberia [in Russian]. Nauka, Novosibirsk, pp. 64–74.

Reznitsky, L.Z., Sklyarov, E.V., Karmanov, N.S., 1998. Eskolaite in metacarbonate rocks of the Slyudyanka Group, southern Baikal region. Dokl. Earth Sci. 363 (8), Part 1, 1049–1053.

Reznitsky, L.Z., Sklyarov, E.V., Suvorova, L.F., Karmanov, N.S., Ushchapovskaya, Z.F., 2005. The Chromite–coulsonite–magnetite solid solution: The first find of a rare variety of spinel in terrestrial rocks. Dokl. Earth Sci. 404 (7), Part 2, 1121–1125.

Reznitsky, L.Z., Sklyarov, E.V., Galuskin, E.V., 2011. Complete isomorphic join diopside–kosmochlor $CaMgSi_2O_6$–$NaCrSi_2O_6$ in metamorphic rocks of the Slyudyanka complex (southern Baikal region). Russian Geology and Geophyscis (Geologiya i Geofizika) 52 (1), 40–51 (51–65).

Roy, D.M., Barks, R.E., 1972. Subsolidus phase equilibrium in Al_2O_3–Cr_2O_3. Nature. Phys. Sci. 235, 118–119.

Ruan, L.-J., Cui, W.-Q., 1997. Mössbauer study of iron in V_2O_3-based PTC ceramics. J. Mater. Sci. Lett. 16 (14), 1231–1232.

Rumyantseva, E.V., Lapshin, S.G., 1986. Mineralogy and geochemistry of alkaline-amphibole propilite and Cr-V micaceous metasomatic rocks in the Onega basin, in: New Achievements in Geological and Metallogenic Studies in Orogenic Areas [in Russian]. VSEGEI, Leningrad, pp. 52–64.

Ryzhov, B.I., Troneva, N.V., Polekhovsky, Yu.S., 1991. V hematite in metasomatic rocks of the Trans-Onega area (Karelia). Izv. AN SSSR. Ser. Geol. 10, 133–139.

Saint-Martin, J., 1977. Geological study and evaluation of the Mounana uranium deposit, Republic of Gabon. Trav. Lab. Sci. Terre. Saint-Jerome, Marseille, Ser. B. 5, 1–78.

Schulze, D.J., Flemming, R.L., Shepherd, P.H.M., Helmstaedt, H., 2014. Mantle-derived guyanaite in a Cr-omphacitite xenolith from Moses Rock diatreme, Utah. Am. Mineral. 99 (7), 1277–1283.

Secco, L., Nestola, F., Dal Negro, A., Reznitsky, L.Z., 2008. Crystal-chemical study of $R\overline{3}c$ natural oxides along the eskolaite–karelianite–hematite (Cr_2O_3–V_2O_3–Fe_2O_3) join. Mineral. Mag. 72 (3), 785–792.

Sergeeva, N.E., Eremin, N.I., Dergachev, A.L., 2011. Vanadium mineralization in ore of the Vihanti massive sulfide base-metal deposit, Finland. Dokl. Earth Sci. 436 (2), 210–212.

Shkol'nik, S.I., Reznitsky, L.Z., Barash, I.G., 2011. Possibility of identification of back-arc paleobasins from high-grade orthometamorphite rocks: Evidence from basic crystalline schists of the Slyudyanka crystalline complex, South Baikal region. Geochem. Int. 49 (12), 1177–1194.

Sobolev, N.V., 1974. Mantle Inclusions in Kimberlite: Implications for the Upper Mantle Composition [in Russian]. Nauka, Novosibirsk.

Sobolev, V.K., Zherdev, P.Yu., Kolodko, A.A., 1993. Eskolaite: the first finding in kimberlite. Mineral. J. 15 (1), 83–85.

Sorescu, M., Xu, T., Wade, C., Burnett, J.D., Aitken, J.A., 2013. Synthesis and properties of V_2O_3–Fe_2O_3 magnetic ceramic nanostructures. Ceram. Int. 39 (7), 8441–8451.

Spry, P.G., Scherbarth, N.L., 2006. The gold–vanadium–tellurium association at the Tuvatu gold–silver prospect, Fiji: conditions of ore deposition. Mineral. Petrol. 87 (3–4), 171–186.

Vasiliev, E.P., Reznitsky, L.Z., Vishnyakov, V.N., Nekrasova, E.A., 1981. The Slyudyanka Metamorphic Complex [in Russian]. Nauka, Novosibirsk.

Vredevoogd, J.J., Forbes, W.C., 1975. The system diopside-ureyite at 20 kbar. Contrib. Mineral. Petrol. 52 (2), 147–156.

Xu, Z., Luo, J., Chuang, K.T., 2008. V_2O_3 anode catalyst for solid oxide fuel cell using H_2S-containing hydrogen. ECS Transactions 11 (20), 1–17.

Yang, J., Meng, F., Xu, X., Robinson, P.T, Dilek, Y., Makeyev, A.B., Wirth, R., Wiedenbeck, M., Cliff, J., 2015. Diamonds, native elements and metal alloys from chromitites of the Ray-Iz ophiolite of the Polar Urals. Gondwana Res. 27 (2), 459–485.

Yoder, H.S., Kullerud, G., 1971. Kosmochlor and the chromite–plagioclase association. Carnegie. Inst. Wash. Yearbook 69, 155–157.

Zdravkov, A.V., Gorbunova, M.A., Koptelova, L.A., Khimich, N.N., 2016. Solvothermal synthesis of nanosized particles of vanadium oxide. Russ. J. Gen. Chem. 86 (2), 219–223.

Zhang, R., Du, C., Wang, Z., Liu, Y., Zai, F., Zu, Z., 1987. The discovery of eskolaite in Dukou, Sichuan. Geol. Rev. 33 (4), 367–371.

Editorial responsibility: O.P. Polyansky